行政院國家科學委員會專題研究計畫 成果報告

固態燃料電池封裝玻璃之合成與性質分析(2/2)
研究成果報告(完整版)

計 畫 類 別 ：個別型
計 畫 編 號 ：NSC 95-2221-E-002-161-
執 行 期 間 ：95 年 08 月 01 日至 96 年 07 月 31 日
執 行 單 位 ：國立臺灣大學材料科學與工程學系暨研究所

計 畫 主 持 人：韋文誠

計畫參與人員：碩士班研究生-兼任助理：陳右儒、陳怡如、蔡居諭

報 告 附 件 ：國外研究心得報告
出席國際會議研究心得報告及發表論文

處 理 方 式 ：本計畫可公開查詢

中 華 民 國 96 年 08 月 14 日

行政院國家科學委員會補助專題研究計畫 成果報告

固態燃料電池封裝玻璃之合成與性質分析(兩年)

計畫類別：■ 個別型計畫
計畫編號：NSC 95－2221－E－002－161
NSC94－2216-E-002-020
執行期間：94 年 8 月 1 日至 96 年 7 月 31 日

計畫主持人：韋文誠教授，台大材料系
計畫參與人員：陳右儒、陳怡如、蔡居諭

成果報告類型(依經費核定清單規定繳交)： ■完整報告
本成果報告包括以下應繳交之附件：■赴國外研習心得報告一份

處理方式：除產學合作研究計畫、提升產業技術及人才培育研究計畫、列管計畫及下列情形者外，得立即公開查詢

執行單位：國立台灣大學材料科學及工程學系

中　華　民　國　九十六年八月十四 日

摘要

本研究為兩年期之計畫，計畫將進行固態燃料電池中金屬(Kovar &Crofer 22)與電解質氧化物(氧化鋯基)之間，用於接合及封裝兩系列玻璃的合成與分析工作。研究內容主要分成四個主題，第一是合成低熔點鉍系及鋇系氧化物玻璃，用於固性封裝，量測並報導兩種玻璃之性質，包括軟化點、潤濕性、電絕緣性等。第二是分析探討不同材料與封裝玻璃之界面反應現象，將採用分析式電鏡，進行微結構定量分析。第三主題是探討玻璃系統在 YSZ/crofer22 介面的接合強度及特性，第四是封裝後之洩漏性質，將在室溫及高溫(600℃)進行測試，將不同材料疊層之組合進行氣體洩漏率及玻璃強度之測試。相關的界面反應動力及分子擴散機制也有深入探討。

關鍵字：固態燃料電池、封裝、玻璃陶瓷、界面反應

ABSTRACT

This is a two years project within three topics. The glass systems, either rigid sealing or compliant sealing functions were developed for planar solid oxide fuel cell operating at 600^{o}C. The application of seals is focus on interface of interconnect (Kovar and Crofer 22) and electrolyte (8Y-YSZ). The first topic is oxide glass synthesis. Three series of sealing glasses, lead glass (PbO-ZnO-SiO_2-B_2O_3) and two lead-free glass systems (Bi_2O_3-ZnO-SiO_2-B_2O_3 and BaO-SiO_2-B_2O_3) were characterized. Thermal and chemical stability, the bonding characteristics, and wetting behavior to yttria stabilized zirconia (YSZ) electrolyte were tested. The second topic is analyzed the interfacial morphologies and composition of the glass-ceramic systems by SEM and EDS. The results were also confirmed by XRD and TEM techniques. The crystalline of the glass and interfacial reaction would affect the ion-conductivity of YSZ. The diffusion of Pb and Bi species in glass and interfacial reaction with YSZ are discussed in this reported as well. The third topic is about the bonding strength of the test bars, which in joint YSZ/Crofer22. The last is the leakage rate of sealing glass system at both room temperature and 600^{o}C (operating temperature). The related interfacial reaction kinetics and molecular diffusion mechanism are also reported in this report.

Keywords: SOFC, sealing, glass ceramic, interface reaction,

「燃料電池封裝玻璃之合成與性質分析」期末報告

大綱 頁次

I. Introduction of Glass-Ceramics Systems for Sealing of SOFC

Glass and glass-ceramic materials are the most common sealants used in SOFC. The glass-ceramic systems can be shaped as easy as a molten glass, and as strong as a polycrystalline ceramics. Several glass-ceramics, e.g. Vycor™, are well known and being widely applied in advanced applications.[1]

There are several stringent requirements in mechanical, chemical and electrical aspects for the selection of a suitable glass or glass-ceramic sealants. Three properties are very fundamental for the glass. One is the **glass transition temperature** (T_g) and the other is the **coefficient of thermal expansion** (CTE) of the glass-ceramics. The glass transition temperature is important to allow the glass to flow sufficiently and to provid an adequate sealing function, while maintaining sufficient rigidity for mechanical integrity (compliant sealing). The coefficient of thermal expansion (CTE) must match other cell components, such as the yttria-stabilized zirconia (YSZ) electrolyte and the interconnect material, to minimize thermal stresses. Finally, the electric resistivity of the glass-ceramics should better be than 10^6 ohm/cm.

Various glasses and glass-ceramics with values of T_g and CTE in target range (~800°C) are shown in Table 1.1 designed for ZrO_2 electrolyte. Many glasses and glass–ceramics contain alkali metal oxides [2,3]. Although they have suitable CTE close to YSZ, the oxides easily react with other fuel cell components and poor electric resistivity. For SOFC applications, alkaline-earth-based (especially the BaO) boro-silicate glasses are more commonly used. It has been shown to operate at higher temperature (800°C) more that 1000 h without significant degradation.[4] The

---

[1] Chapter 8 in Fundamentals of Ceramics, by Michel Barsoum, McGraw-Hill Series in Mat. Sci. and Eng., Int. Ed. 2000

[2] K. L. Ley, M. Krumpelt, R. Kumar, J. H. Meiser, and I. Bloom, *J. Mater. Res.*, 11 (1996) 1489-1493

[3] H. Rawson, *Properties and Applications of Glass*, Ch 3 & Ch 8, Elsevier Science Publishing Company Inc., 1980

[4] J. Fergus, Sealants for solid oxide fuel cells, *J. Power Sources*, 147 (2005) 46-57

examples of detail analysis of the composition on the T_g, wetting angle, strength, CTE, and leak rate of gas are given by Fergus.[4]

Table 1.1 Glass and glass-ceramic of silicates sealants used for various temperature ranges

All designed for matching ZrO_2 electrolyte				
Composition	Properties		Characteristics	Ref.
	T_g (^oC)	CTE (ppm/^oC)		
$BaO-Al_2O_3-SiO_2-B_2O_3$	610~670	9.3~12.8	Thermal properties can be adjusted with NiO, ZrO_2, and La_2O_3. CTE may change by crystallization. B_2O_3 volatizes with water vapor.	5 6
$BaO-Al_2O_3-SiO_2$	690~720	10.5~11.4	The most popular system in sealing field. CTE value decrease due to crystallization. Doped MgO is able to control the rate of crystallization.	7
$BaO-SiO_2-B_2O_3$-RO (R=Ca, Mg, Zn)	625~660	10.5~11.4	Have suitable thermal properties, but rapidly crystallization.	4
$SrO-La_2O_3-Al_2O_3-B_2O_3-SiO_2$	560-760	7.5-11.5	High T_g system, CTE value decrease due to crystallization	8
$BaO-SiO_2$-RO (R=Mg, Zn)	673~721	10.5~12	Lower BaO/RO ratio have better sintering/crystallization for obtaining suitable glass-ceramics. But have lower CTE value.	9
$SiO_2-Al_2O_3$- CaO-MgO-RO	??	OK	For sealing plates	10
NiO-ZrO_2-CoO-CaO-SrO-meta	??	??	Sealing and gap filler	11

[5] S. Sohn, S. Choi, G. Kim, H. Song, and G. Kim, *J. Am. Ceram. Soc.*, 87(2004) 254-60.
[6] S. Sohn, S. Choi, G. Kim, H. Song, and G. Kim, *J. Non-Cryst. Solids*, 297 (2002) 103-112
[7] C. Lara, M. J. Pascual, and A. Duran, *J. Non-Cryst. Solids*, 348 (2004) 149-155
[8] US patent 5,453,331 (Univ. of Chicago) Sep. 26, 1995
[9] C. Lara, M. J. Pascual, M.O. Prado, and A. Duran, *Solid State Ionics*, 170 (2004) 201-208
[10] C. Thompson, A. Wood, S. Pyke, US patent 6,656,625, Alstom UK Ltd. (GB)
[11] L. A. Xue, Bonding Mat. for Anode to Anode bonding and to interconnect bonding in SOFC, US patent 5,702,837

l filler				
Bi_2O_3-ZnO-B_2O_3-ZnO	450	11.9	CTE value decrease due to crystallization and higher electrical conductivity	12, 13
MgO-Al_2O_3-P_2O_5	600	4.5~5.6	The CTE value is too low for application	14
MgO/CaO/Cr_2O_3 - Al_2O_3-B_2O_3-P_2O_5	600-630	5.7-7.9	CaO content determined interface reaction and	15
Fe_2O_3-P_2O_5-(Al_2O_3, SiO_2, B_2O_3)	500~510	4.5	The CTE value is too low for application	16
60SnO-10MgO-30P_2O_5-B_2O_3	?	11	Doped with 6~50 mol% B_2O_3 will rise CTE to 11ppm/K	17
CaO-B_2O_3-SiO_2	?	?	Sintering temperature at 875^oC	18
Mica/SiO_2-B_2O_3-Al_2O_3-BaO	?	11	Doped more than 10% mica will lower CTE of glass	19

Only five US patents have been found relating to the sealing glasses used for SOFC (Table 1.2). They have the claims covered the glass compositions and the applications that are similar to previous study. The oxide ingredients are mainly silicate, doped with ZnO- or the other alkaline-earth oxides. It is difficult without infringing on the formulation ranges and claims of those patents.

Table 1.2 US patents with the claims on sealing glass for SOFC

US Patent no.	Glass composition	Claims	Assignee
6,656,625	**Si-Ca-Mg-Al-oxides** SiO_2 (43-59wt%), Al_2O_3(5-7%) CaO (10-20.8%), MgO (0-30%) or BaO (0-36.3%), or TiO_2 (4%)	Good CTE match up to 1000^oC	Alstom. UK
6,291,092	**MO-Zn-Si-oxides** SiO_2 (50-70 wt%), ZnO (10-25%) K_2O (5-15%), Na_2O (2-10%) Ba, Ti, Zr,-oxides (0-10%)	600-1000^oC application temperature	Corning
6,271,158	**Corning 4060 or 3103 glasses**, SiO_2 (50-70 wt%), ZnO (10-25%) K_2O (5-20%), Na_2O (1-15%) Li, Ba, Zr, Ca, Mg-oxides (0-8%)	A mixture of glasses (>40 wt%) with metal (Ni, Fe,	AlliedSignal

[12] I. Dyamant, D. Itzhak, and J. Hormadaly, *J. Non-Cryst. Solids*, 351 (2005) 3503-3507
[13] Y. J. Chen "Investigation of Vapor Phase Thin Film Deposition and Interfacial Reaction in Bismuth Oxide Glass/YSZ System", (2006) NTU MS thesis
[14] P. H. Larsen, F.W. Poulsen, and R. W. Berg, J. Non-Crystalline Solid, 244 (1999) 16-24
[15] P. H. Larsen, and P. F. James, J. Mat. Sci., 33 (1998) 2499-2507
[16] P.A. Bingham, R.J. Hand, and S.D. Forde, J. Mat. Res. Bulletin, 41 (2006) 1622-1630
[17] C. C. Hsieh, and. J. J. Shyu, Taiwan Ceram. Soc. Conference, (2007) 156
[18] C. C. Chiang, S. F. Wang, Y. R. Wang, and Y. F. Hsu, Taiwan Ceram. Soc. Conference, (2007) 161
[19] C. K. Liu, T. Y. Yung, and K. F. Lin, Taiwan Ceram. Soc. Conference, (2007) 147

		Cr) particle	
5,702,837	**Ni-Zr-Co-Ca-Sr-oxides** with W, Ta, Nb, Mo, Ti reactive metal ingredients	Slurry formulation for anode-anode bonding	AlliedSignal
5,453,331	**La-Sr-Al-Si-B-oxides**, SrO (5-60%) -La_2O_3 (0-45%) -Al_2O_3 (0-15%)-B_2O_3(15-80%) -SiO_2 (0-40%) or Ca-Al-B-Si-oxides	Wide range of T_g and CTE matching to YCZ	Univ. of Chicago

Objectives:

1. Find a glass-ceramic system with T_g in between 600 to 750^oC, therefore, can be applied for the SOFC at the operation range of 800-850^oC, which is the application temperature of bulky 8Y-SZ; (refer to Fig. 1.1)
2. Find a glass-ceramic system with T_g between 450 to 600^oC, therefore, can be applied for the SOFC at the application range of 800-850^oC, which is the application temperature range of ultra-thin 8Y-CSZ electrolyte. [20](refer to Fig. 1.1)
3. Fully characterize the material properties of above two glass-ceramic systems.
4. Study the interface microstructure of above two glass-ceramic systems next to the YSZ electrolyte;
5. Study the interface microstructure of above two glass-ceramic systems next to selected metal alloys, including Kovar and Crofer 22.

[20] Y. Y. Chen and W. J. Wei#, 2006, "Processing and characterization of ultra-thin yttria stabilized zirconia (YSZ) electrolytic film for SOFC," Solid State Ionics, 177, [3-4] pp. 351-357, NSC92-2212-E-002-097 and the NSC-DAAD summer program of 2002

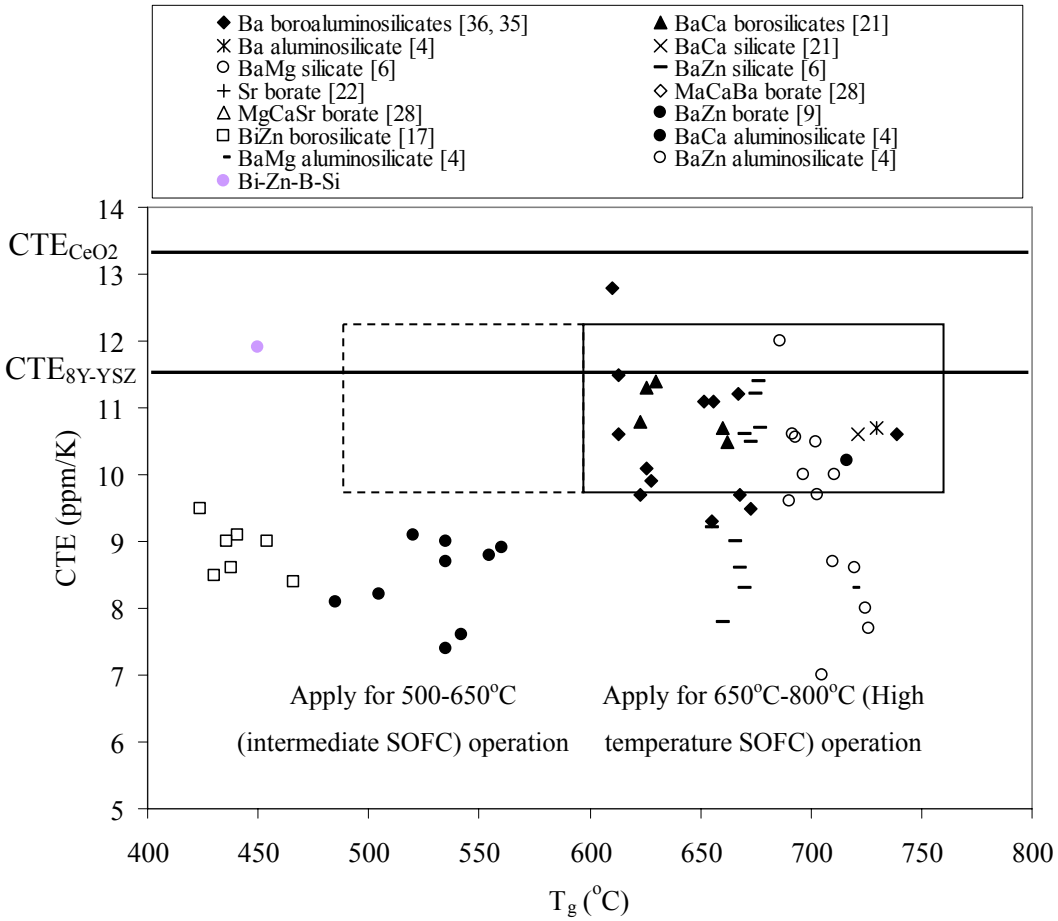

Fig. 1.1 Glass transition temperature (T_g) and coefficient of thermal expansion (CTE) for SOFC sealant materials. The solid-line rectangle represents the favor range for a higher-operation-temperature SOFC; the dash-line rectangle represents the favorable range for an intermediate operation temperature SOFC.

II. Bi- and Pb-glass Ceramic Systems

The whole purposes in this section is mainly to find a glass system that can be used for the SOFC applied below 500<<650^{o}C. The experimentals and tasks could be separated into four parts and listed below:

- preparation of glasses;
- glasses and glass-ceramics characterization (crystalline phase, thermal properties, and electrical conductivity);
- bonding, wetting, and interfacial chemical reaction; creeping behavior analysis
- Creeping behavior of glass-ceramics

2.1 Preparation of Bi- and Pb-glasses

Seven commercial glass powders were purchased from Exojet Technology Corporation (技嘉科技). One glass GP-014 (assigned P1) having desirable properties was fully characterized and reported in this report. The main composition of this glass is PbO, ZnO, SiO_2 and B_2O_3, average particle size is 1.94 μm (Table 2.1). Inductively coupled plasma (ICP, Jobin Yvon) was employed to analysis the compositions of Pb-glass. Besides, Bi_2O_3 was used to substitute PbO. In previous report the glass transition temperature (T_g) strongly dependent on B_2O_3/SiO_2 ratio. Because P1 glass has a lower T_g, we reduced B_2O_3/SiO_2 ratio to 0.25-0.50 in order to raise T_g.

Table 2.1 One PbO-commercial glass and Bi-Zn-Si-B glass compositions

Glass	Composition (mol%)				
	PbO	ZnO	SiO_2	B_2O_3	B_2O_3/SiO_2
P1	35.42	39.14	8.07	17.36	2.15
	Bi_2O_3	ZnO	SiO_2	B_2O_3	B_2O_3/SiO_2
B1	35.42	39.14	16.69	8.48	0.5
B2	25	25	33.33	16.66	0.5
B3	25	25	40	10	0.25
B4	30	20	40	10	0.25

Literature review has assured that there is no quaternary phase diagram, only two ternary phase diagrams Bi_2O_3-ZnO-SiO_2 and Bi_2O_3-ZnO-B_2O_3 available, as shown in Fig. 2.1.

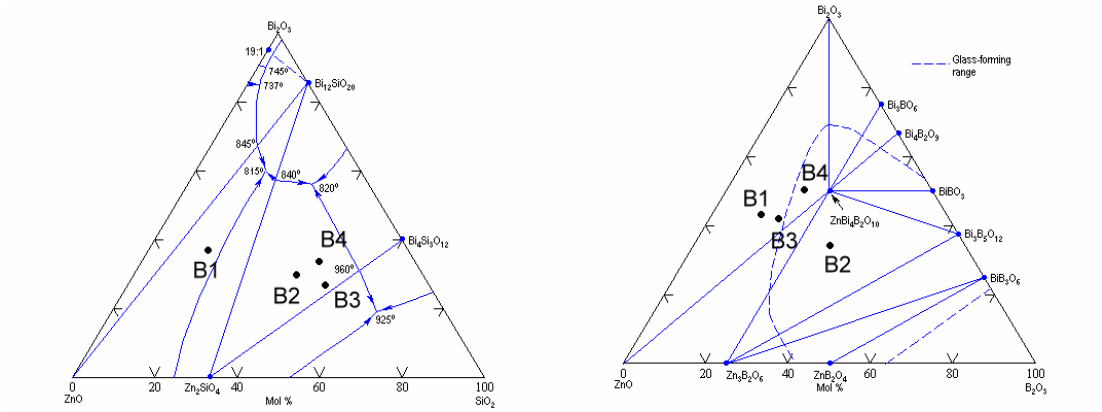

Fig. 2.1 Ternary phase diagrams Bi_2O_3-ZnO-SiO_2 and Bi_2O_3-ZnO-B_2O_3.

Bi-glasses were synthesized from analytical grade fused silica, Bi_2O_3, ZnO and H_3BO_3. Batch formulations were calculated to produce 50 g glass sample in Pt crucible. An electric furnace was used for melting the batches at temperature 1200°C and quenched with water. The glasses were ground using an agate and sieved through a sieve of 150 mesh. Pellets were made by die-pressing of granulated glass powder.

The design of this work required only the sealing between the electrolyte and interconnect. Yttria-stabilized zirconia is a common material used as SOFC electrolyte. The YSZ plates were prepared from 8 mol% YSZ (TEAMCera, Taiwan) by pressure filtration, sintering, and polishing.

2.2 Characterization of the Glass-Ceramics

The as-prepared glasses were analyzed by X-ray diffractometry (Philips PW 1972, Philips Instrument, Netherlands) with Cu Kα radiation to confirm the amorphous nature of glass.

The thermal properties of the glasses, such as glass transition temperature (T_g) and crystallization temperature (T_c) were measured using differential thermal analysis (DTA, DuPont, 1600DTA) in air at a heating rate of 5°C/min. CTE values of glass and glass-ceramic were measured by TMA (TMA 2940 Thermo-mechanical Analyzer (TA), DuPont, USA)

After thermal treatments glass-ceramic were characterized using XRD and scanning electron microscopy to investigate the crystallization behavior of the glasses. XRD measurements were performed to identify the precipitated crystalline phases and to observe the development of crystalline phases, which were evaluated from the comparison of the relative intensities of the largest peaks corresponding to each phase in the XRD patterns. SEM (Tungsten, Philips XL30,) observation on the polished surface of heat-treated glass was conducted to investigate microstructure changes causing by crystallization and at operation temperature.

The electrical conductivities were measured by two-probe measurement, from room temperature to T_g.

2.3 Results of Lead and Bismuth Oxide Serials Glasses

The thermal properties of glasses were analyzed by DTA and shown in Table 2.2. P1 glass has a lower T_g and T_c, because of higher B_2O_3 content and melt at 630 ^oC.

In Bi_2O_3 glass system, T_g will decrease with increasing the concentration of Bi_2O_3. The B4 glass has higher T_g and T_c suitable for the requirement of SOFC sealing application. But if heat-treated at 650^oC for more than 1 hr, crystallization of $Bi_4(SiO_4)_3$, $Bi_{12}SiO_{20}$, and Zn_2SiO_4 will appear and lower down the CTE value to 4 ppm/K.

Table 2.2 Glass transition temperature (T_g), crystallization temperature (T_c), and coefficient of thermal expansion of glass.

Glass	T_g (^oC)	T_c (^oC)	CTE (ppm/K)
P1	400	490	9.1
B1	394	535	10
B4	460	575	11.9

2.3.1 Properties of the Pb-Glass Ceramics

P1 glass shows a good wetting on YSZ at 650^oC (Fig. 2.2). Fig. 2.3 shows the cross-section of the glass P1/YSZ interface heat-treated at 650^oC. At first 1 hr shown in Fig. 2.3(a), there is no significant inter-diffusion between glass/YSZ. But Pb had shown significant diffusion at >10 hr. Because the coordination number and ionic radius of Pb^{2+} are small, the Pb^{+2} easily diffused into YSZ and reacted with ZrO_2 to form $PbZrO_3$. At 100 hr, the diffusion distance of Pb^{2+} could reach 100 μm.

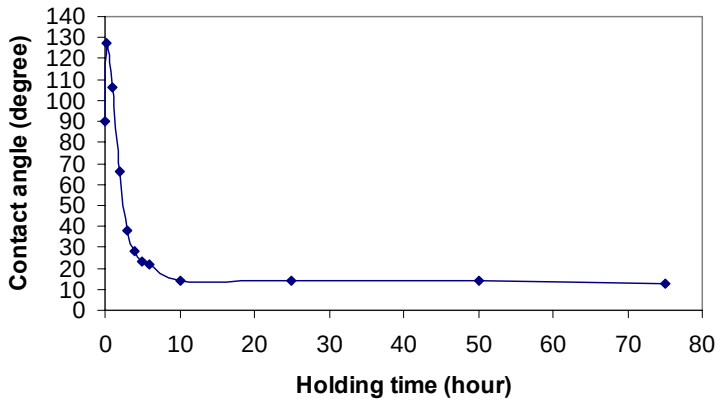

Fig. 2.2 Contact angle of glass P1 heat-treated at 650^oC for various times

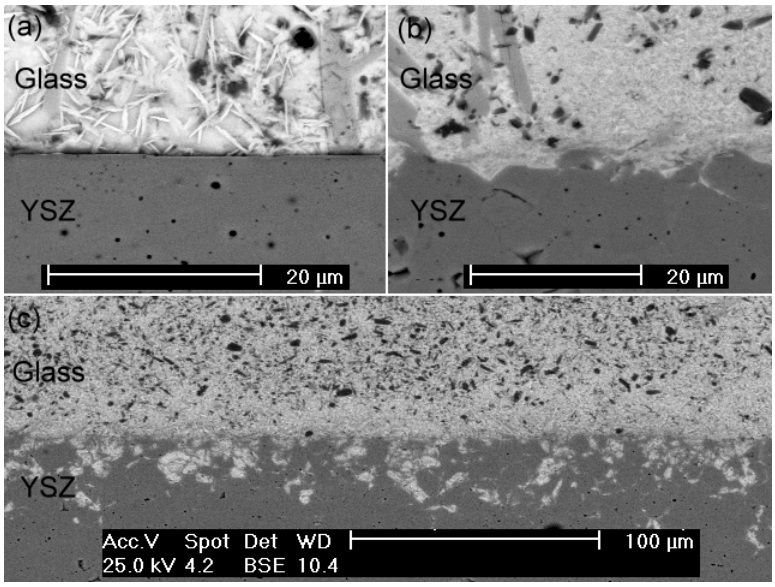

Fig. 2.3 SEM cross-section views of glass P1/YSZ interface heat-treated at 650°C for (a) 1, (b) 10, and (c) 100 hr.

Fig. 2.4 shows the XRD patterns of glass P1 heat-treated at 650°C for various periods. The specimen of as-prepared glass powder exhibited a broad intensity in XRD pattern. After 10 min and 10 hr heat-treated at 650°C, the glass exhibited poor crystallinity.

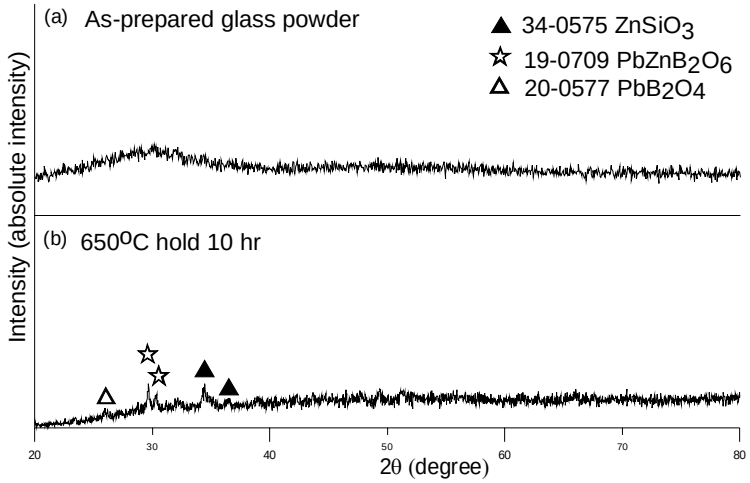

Fig. 2.4 XRD patterns of as-prepared P1 glass and heat-treated at 650°C for 10 hr.

In brief, P1 glass has a low melting point (630°C) and the Pb^{2+} in the glass would diffuse into YSZ to form $PbZrO_3$, poisoned electrolyte. It is not suitable as SOFC sealing glass.

2.3.2 Properties of Bi-Glass Ceramics

In Bi-glass system, B4 has better thermal properties matching to SOFC requirement, and has a better junction with YSZ.

(a) Bonding, Wetting, and Interfacial Chemical Reaction

The operation temperature of a thin electrolyte SOFC[20] is between 575-750°C, so the operation temperature in this investigation was set at 600°C and with acceleration test at 650°C up to 100 hr.

The bonding characteristics and wetting behavior of the glass to YSZ and to Kovar were examined by observing the wetting behavior of the glass. The chemical reactivity between the YSZ, glass-ceramic, and Kovar were investigated using heat-treatment up to 100 hr at 650°C. After the heat treatment, a cross section of the specimen was polished, and the interface between the glass-ceramics and the YSZ then was examined using SEM (Philips XL30) with EDS (EDS, England) to investigate chemical reactivity and microstructure change at the interface as a result of a long-term operation. No boron could be detected by the EDS instrument. Consequently, boron was not reported in the following results.

The wetting behavior of the glass was investigated by observing shape change of the bulky cylinders on YSZ plate at increasing temperature. The shape change of the cylinders might be affected by the glass viscosity and fluidity, the glass normally underwent crystallization and melting simultaneously. The results (Fig. 2.5) show that the glass starts to wet on YSZ substrate as the temperature reaches 930°C.

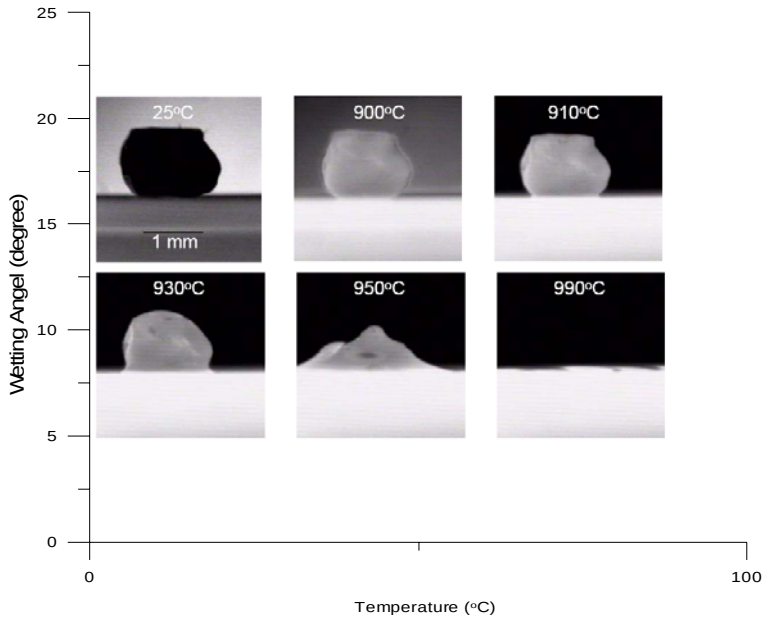

Fig. 2.5 Shape change of glass bulk specimen at various temperatures (heating rate: 5°C/min).

In order to develop a good sealant, it is necessary to understand the crystallization behavior, sealing properties, and long-term stability at applied temperature. Fig. 2.6 exemplified the XRD patterns of the B4 glass powder and treated at 650°C. The spectra of the as-casted glass exhibited broad diffraction intensity in the XRD pattern.

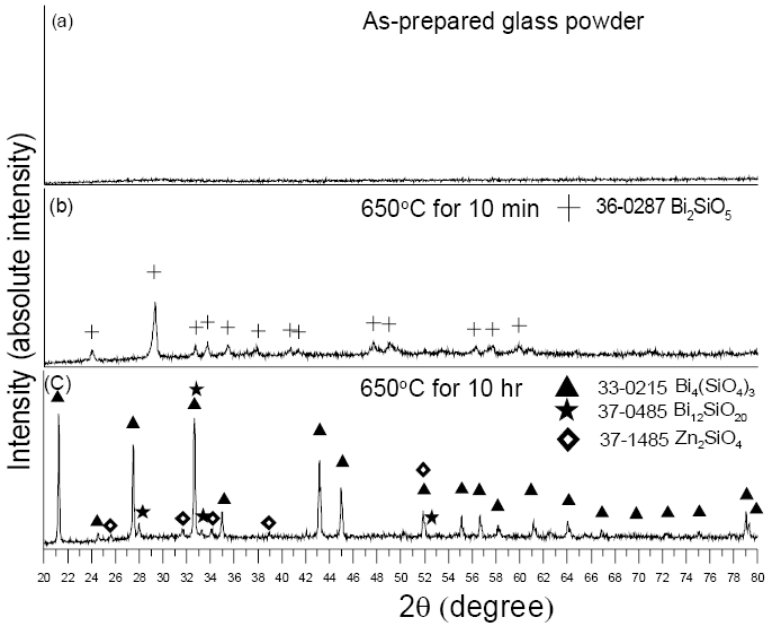

Fig. 2.6 XRD patterns of glass B4 heat-treated at 650°C for various periods.

At 650°C holding for 10 min, column crystal Bi_2SiO_5 was found to be the main crystalline phase in the glass, as shown in Fig. 2.6(b). As the holding time was longer than 1 hr, Bi_2SiO_5 dissolved into glass phase and re-crystallized into $Bi_4(SiO_4)_3$, $Bi_{12}SiO_{20}$, and Zn_2SiO_4 (Fig. 2.6(c)). Detail micro-observation showed four crystalline phases in Fig. 2.7(a). It is believed that all B_2O_3 content due to its glass forming ability forms the glassy boundary with Bi_2O_3 and ZnO ingredients.

The diffusion of Bi-species into ZrO_2 is noted in Fig. 2.8(b) along YSZ grain boundary, especially the interface without the growth of Zn_2SiO_4 crystals. The Zn_2SiO_4 layer next to ZrO_2 seems play a role to block the transport of the Bi-B-Zn-O glass. The depth of the diffusion is limited to a few micrometers as holding for 10 hr. The maxima diffusion depth of the sample was 8 μm in average. The crystallization reaction sequence of the glass is proposed as follows. Bi_2O_3, ZnO, SiO_2 and B_2O_3 react at 650°C, only the Bi_2SiO_5 phase exists at the first moment. The other elements forms glass phase in small quantity in the matrix, but still not able to creep at this temperature. As the time extends, the Bi_2SiO_5 phase either dissolves into the glass phase, then re-crystallizes a new phase $Bi_4(SiO_4)_3$. During the crystallization, both Bi_2O_3 and ZnO in borosilicate glass had shown different diffusive results in YSZ. The

YSZ grains could act as the nuclei for the growth of Zn_2SiO_4 crystals. The formation of the nuclei explains the preferential growth of the crystals at the interface. The diffusion of Bi-species was analyzed, as shown in Fig. 2.8. The results of lattice diffusivity are 1.3615×10^{-17} m^2/s and grain boundary diffusivity is 4.1×10^{-8} m^2/s.

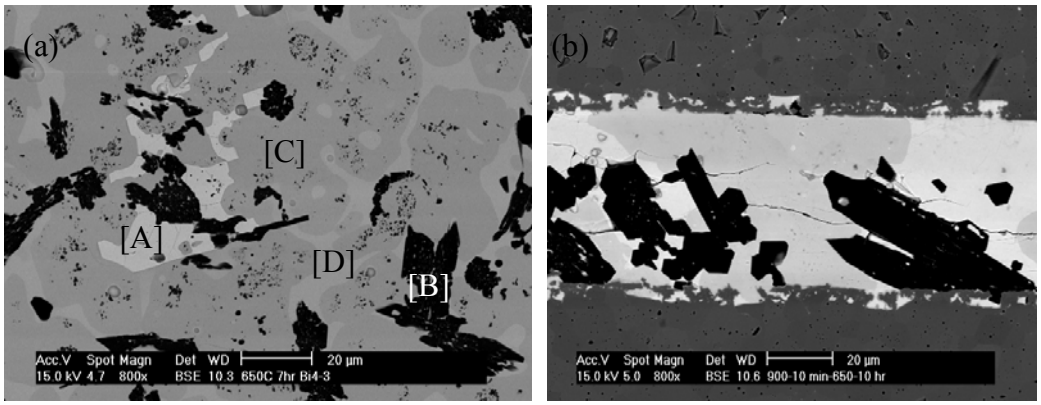

Fig. 2.7 (a) SEM morphology of B4 glass heat-treated at 650°C for 7 hr. [A] represents the crystalline phase $Bi_{12}SiO_{20}$, [B] represents the phase Zn_2SiO_4, [C] represents the phase $Bi_4(SiO_4)_3$, and [D] represents the glass phase. (b) SEM cross-section micrograph of glass/YSZ interface, which was heat-treated at 650°C for 10 hr.

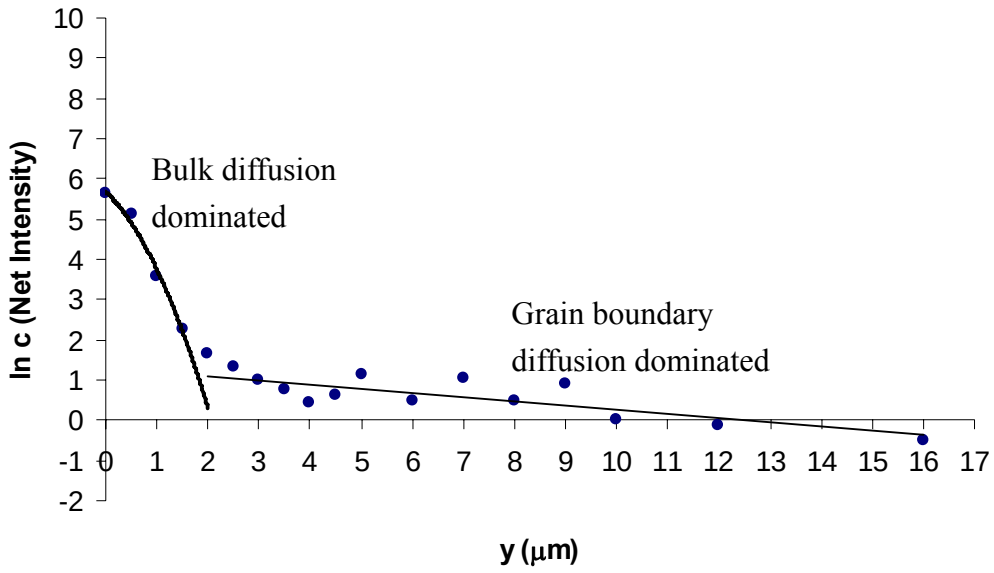

Fig. 2.8 Diffusion profile of B4-glass/YSZ after a heat treatment at 650°C for 10 hr. There are two regimes of bulk diffusion and grain boundary diffusion.

(b) Electrical conductivity. Fig. 2.9 shows the conductivity versus temperature of B4-glass after a heat treatment at 650°C for 10 hr. There are two best-fitted slopes

shown in Fig. 2.9. The activation energy of B4-glass below T_g is 1.77 eV.

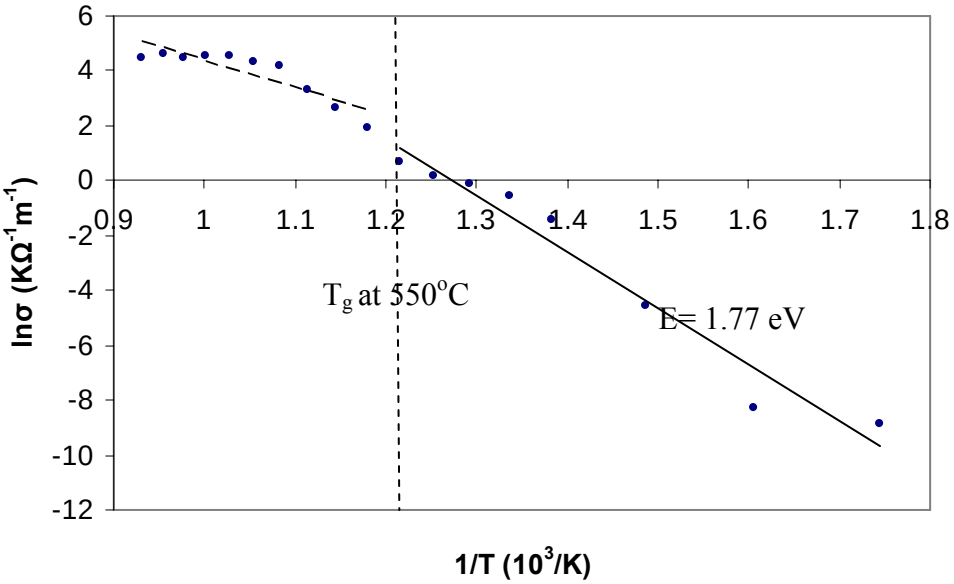

Fig. 2.9 Conductivity versus temperature of B4-glass after 650°C for 10 hr heat treatment (sample diameter=5.4 mm and thickness=0.98 mm).

(c) Creeping behavior analysis. TMA (DTA, DuPund, 1600DTA) was employed to analyze the creeping behavior of glass. All samples were measured in air with a heating rate of 5°C/min. Fig. 2.10 shows the creeping behavior result of as-crystallized YSZ/glass/YSZ sandwich sample at 750, 700 and 650°C with a heating rate of 10°C/min and 8.5 kPa loading. The creeping rate is higher as the temperature is higher. A creeping rate (0.114 μm/hr) at 650°C supply sufficient viscous flow to healing the cracks. The viscous flow of glass can explain this phenomenon[1].

The creep rate was proportional to temperature. The viscosity can be estimate by eq. (1) [2-3].

$$\eta = \frac{\sigma}{2(1+\upsilon)\dot{\varepsilon}} = \frac{\sigma}{3\dot{\varepsilon}} \quad \text{.....(1)}$$

The results of apparent viscosity are listed in Table 3, where σ is the applied stress. The unit of σ is Pa. ε is the strain rate measured during creep tests and υ is the Poisson's ratio of glass bulk.

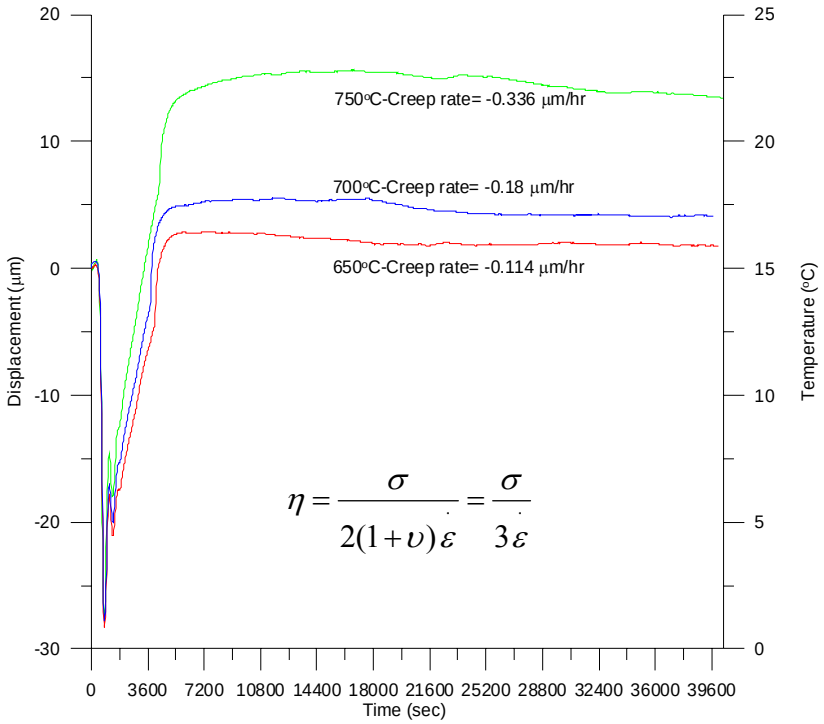

Fig. 2.10 Creep behavior of YSZ/glass/YSZ sandwich samples at 750, 700, and 650°C for 10 hr with a 8.5 kPa load.

Table 2.3 Viscosity of Bi-glass at different heat-treated conditions.

Sample condition	Load (kPa)	Apparent viscosity (Pa·s)	Viscosity of glass (Pa·s)
750°C pre-crystallized	8.5	3.04×10^9	3.2×10^5
700°C pre-crystallized	8.5	5.68×10^9	6×10^5
650°C pre-crystallized	8.5	8.97×10^9	9.49×10^5

The degree of crystallization in the glass affects the viscosity. It changes with the amount, the size and shape of crystals, which has been described as below [4-5]:

$$\eta = \eta_0 (1 - f)^m \quad \text{.....(2)}$$

$$m = \frac{3F - 2}{3F(1 - 2F)} \quad \text{.....(3)}$$

where η_0 is the viscosity of the glass, f is the volume fraction of the crystals (inclusions) and m is a constant, a function of the shape of crystals. F is the shape factor. The calculations of apparent viscosity are listed in table 2.3.

2.3.3 Interface Reaction with Kovar and Crofer 22

Bismuth oxide based glass has a large amount of reaction with Kovar comparing

with YSZ shown in Fig. 2.11, and the diffusion analysis of glass between YSZ and Kovar, as shown in Fig.11. A porous oxidization layer formed at alloy surface, which has lower joining strength, cracked during sample preparation. Large amount of Fe-rich crystals were caused by FeO diffusing into the glass and inducing crystallization. It needs surface coating on Kovar surface to prevent oxidization and supply better joining strength.

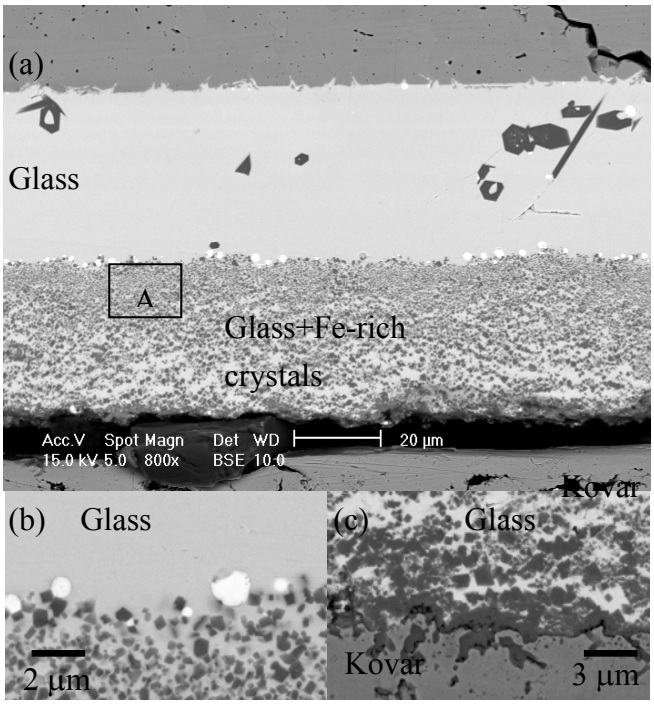

Fig. 2.11 (a) SEM (backscattering mode) cross-section micrograph of YSZ/glass/Kovar interface, which was heat-treated to 950°C joining with YSZ and Kovar for 10 min and quenched. (b) Higher magnification of point A. (c) Higher magnification of glass/Kovar interface.

Fig. 2.12 shows the cross-section of B4-glass jointed with Crofer 22 at 650°C with 10 hr heat-treated. Although there is no apparent oxide layer of Crofer 22 being observed, CTE mismatch induced a crack along the interface. There are also cracks inside the glass-ceramic body. So B4-glass/Crofer 22 appeared a weak bonding, needed improvement by reducing CTE mismatch, of which doped with ZrO_2 will be reported in next section.

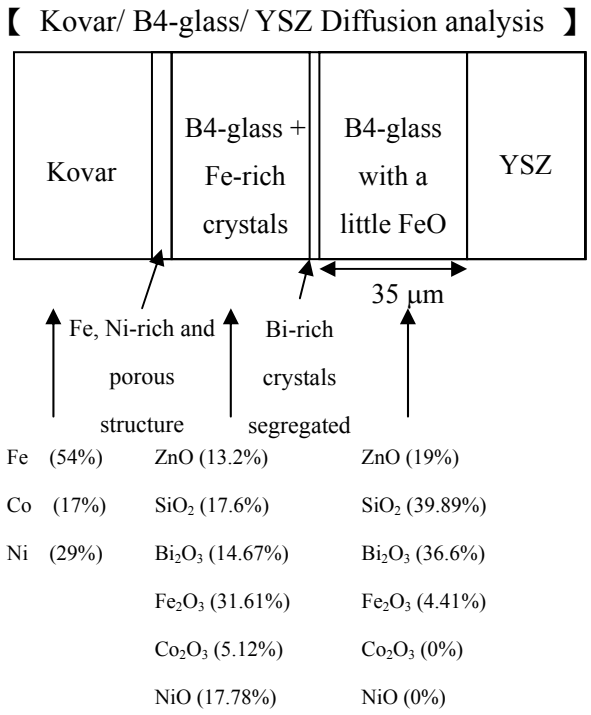

Fig. 2.12 Schematic diagram of diffusion analysis between Kovar/glass/YSZ.

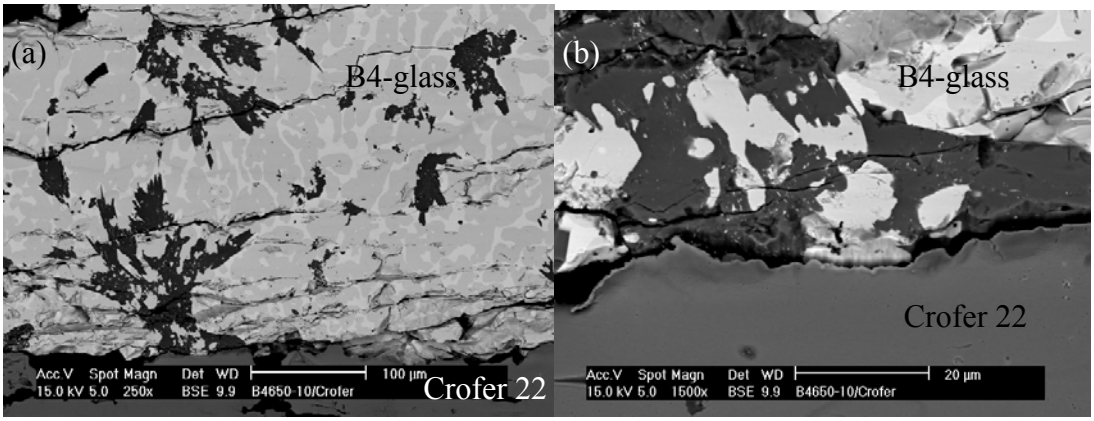

Fig. 2.13 SEM cross-section images of B4-glass joint with Crofer 22 at 650°C with 10 hr heat-treated.

2.3.4 Modification of B4 Glass System

B4 glass shows good thermal properties at glass state, but not at glass-ceramic state. We expected to modify this system in CTE properties by doping 0Y-ZrO_2. Pure 0Y-ZrO_2 has CTE property close to the other components in SOFC and shows a lower electrical conductivity. Fig. 2.14 shows the microstructure of the B4 glass with 30 wt% ZrO_2 holding at 650°C for 10 hr or 100hr. The dopant ZrO_2 can raise the CTE of B4Z30 glass-ceramics to a CTE value of 10 ppm/K.

Fig. 2.15 shows the XRD results of B4-doped ZrO_2 samples with different

annealing periods. Four crystalline phases, including $ZrSiO_4$, $Bi_{12}SiO_{20,}$ Bi_2SiO_5, and $Bi_4ZnB_2O_{10,}$ were identified in the sample by 10 hr heat treatment. As the treatment extending to 100 hr, a new phase $Bi_{7.38}Zr_{0.62}O_{12.31}$ grown from glass phase was observed, which would lowered down the CTE value.

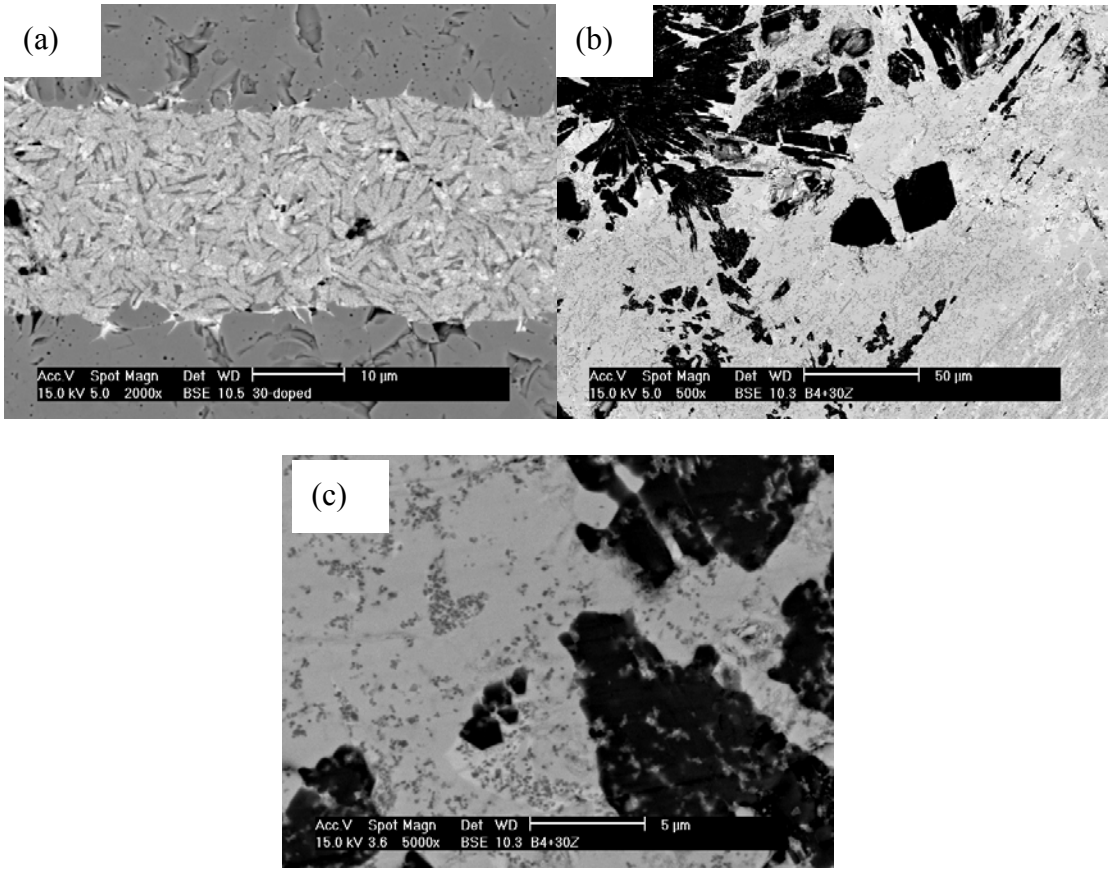

Fig. 2.14 SEM cross-section images of 30 wt% ZrO_2 doped B4-glass with 650^{o}C (a) 10 hr and (b) 100hr heat-treated. (c) The higher magnification of 100 hr-treated sample.

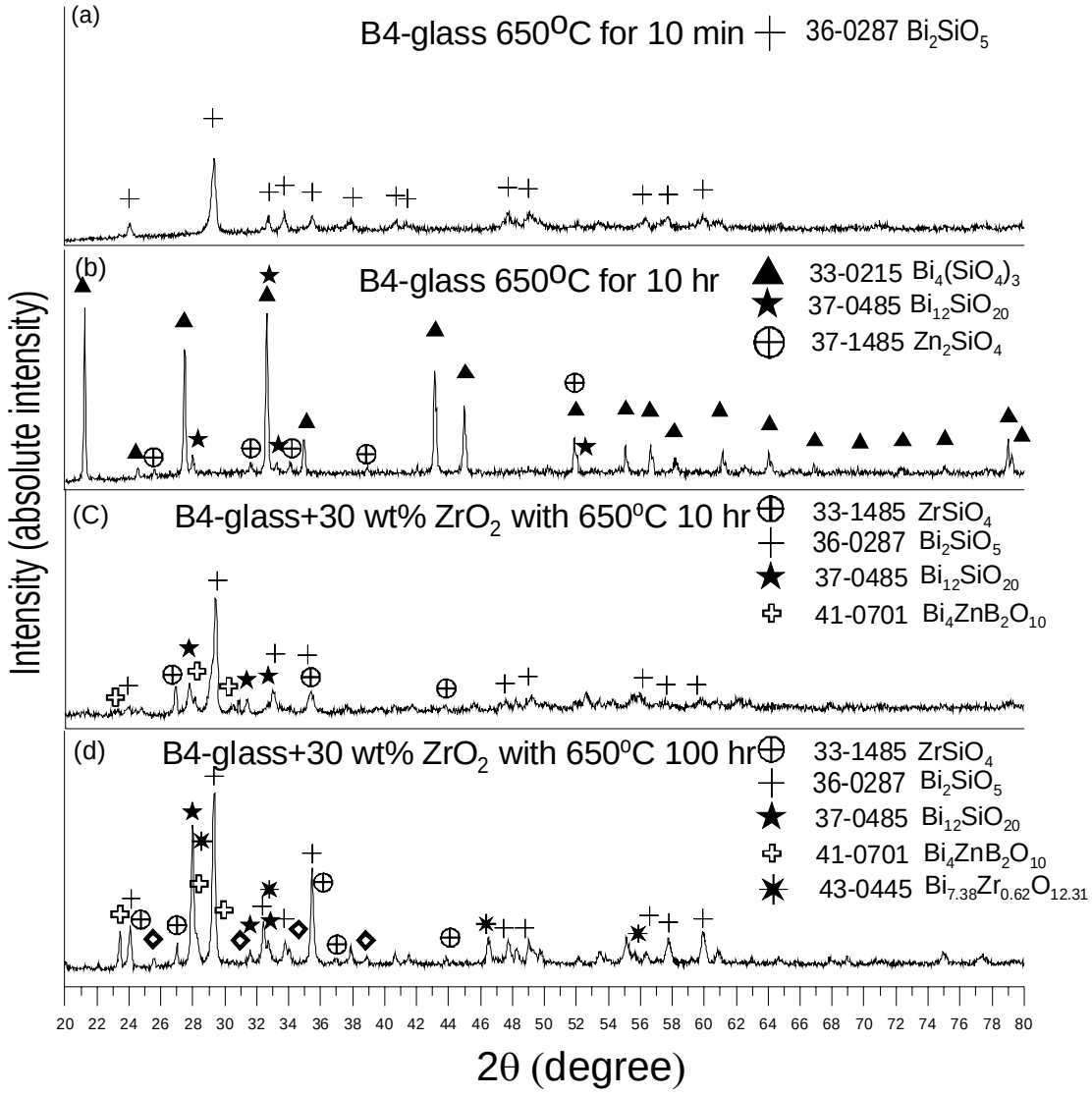

Fig. 2.15 XRD results of B4-glass and B4-doped 30 wt% ZrO_2 sample with different annealing time. (a) B4-glass at 650°C for 10 min, (b) B4-glass at 650°C for 10 hr, (c) B4-doped 30 wt% ZrO_2 sample at 650°C for 10 hr, and (d) B4-doped 30 wt% ZrO_2 sample at 650°C for 100 hr.

III. Ba-glass Ceramic Systems

Currently, glass-ceramics are the preferred materials in these restrict requirements for sealing SOFC stacks. With an effort to develop such a suitable sealant for planar SOFCs, borosilicate, boron-free alkaline earth silicates, and phosphorus silicate had been suggested in many scientific articles for SOFC sealing applications. Because P_2O_5 not only increases the crystallization tendency in most silicate glass for the long-term stability concerns, but also the phosphorus silicates exhibit low CTE value of 5-6 ppm/K, too low to be a good candidate. Neither boron-free alkaline earth silicates were considered because of its high viscosities. Consequently, the present work would emphasize on borosilicate glass-ceramics.[21]

3.1 Experiment of Ba-Glass Preparation

3.1.1. Glass preparation

To prepare a suitable sealing glass, B_2O_3 and SiO_2 were chosen as a glass former. As Sohn *et al.* mentioned that B_2O_3 can decrease the viscosity and crystallization tendency of glasses. With increasing the B_2O_3/SiO_2 ratio, the CTE of the sealing glasses also increase[22]. Other component, BaO, as network modifier, can increase the CTE value and show a better glass formation ability with decreasing phase separation tendency. Al_2O_3, as an intermediate additive, can prevent rapid crystallization of a glass during heat-treatment and also to increase the surface tension of glass. [23,24,25]

The composition of the glass listed in Table 3.1 were prepared by taking stoichiometric amounts of reagent-grade $BaCO_3$, H_2BO_3, SiO_2, and Al_2O_3, then milling thoroughly in a turbo-mixer for 24 h in alcohol (10 vol%).

---

[21] A. Fluegel, " Sealing Glass-Ceramics for Planar Solid Oxide Fuel Cells Literature Review," http://glassproperties.com/sofc/, (2005)

[22] S.-B. Sohn, S.-Y. Choi, G.-H. Kim, H.-S. Song, and G.-D. Kim, "Stable Sealing Glass for Planar Solid Oxide Fuel," J. Mat. Sci., 297, 103-112 (2002)

[23] J. W. Fergus, "Sealants for Solid Oxide Fuel Cells," J. Power Sources, 147, 46-57 (2005)

[24] Gyeung-Ho Kim, Hue-Sup Song, Goo-Dae Kim, "Suitable Glass-Ceramic Sealant for Planar Solid-Oxide Fuel Cells," J. Am. Ceram. Soc., 87[2], 254-260 (2004)

[25] K. S.Well, J. E. Deibler, J. S. Hardy, D. S. Kim, G. G. Xia, L. A. Chick, and C. A. Coyle, "Rupture Testing as a Tool for Developing Planar Solid Oxide Fuel Cell Seals, " J. Mater. Sci. Perm., 13, 316-326 (2004)

Table 3.1 Chemical composition and thermal properties of the glasses used in this work

Specimen	Composition (mol%)					Thermal Properties(^{o}C)	
	BaO	B_2O_3	SiO_2	Al_2O_3	B_2O_3/SiO_2	T_g	T_c
G0	50	25	25	—	1	534	580/668/712
G1	50	22	28	—	0.78	554	669/700
G2	50	17	33	—	0.52	556	661/694
G3	50	12.5	37.5	—	0.33	568	668
G4	50	10	40	—	0.25	572	640
G0A5	47.62	23.81	23.81	4.76	1	585	787
G1A10	45.45	20	25.45	9.09	0.78	625	828/1074/1226

The mixed batches were melted in an electric furnace at 1300^{o}C for 30 min in a Pt crucible, and then poured onto a graphite plate to form a glass bulk or quenched glass into 25^{o}C de-ionic water. The water-quenched glasses, then, were ground and sieved through 150 meshes in order to obtain fine glass powder.

3.1.2. Glass Characterization

The as-prepared and heat-treated glasses were analyzed by X-ray diffractometry (Philip PW 1972, Philips Instrument, Netherlands) using Cu K_α radiation to confirm the amorphous nature and crystalline phases of the glass-ceramics.

The measurement of the glass properties that might influence sealing, such as glass transition temperatures (T_g) and crystallization temperatures (T_c), was performed by using Differential Thermal Analyzer (1600DTA, DuPont Instrument, Germany) with a Pt crucible as the sample holder and α-Al_2O_3 powder (been calcined at 1200^{o}C) as inert reference. DTA scans were recorded from room temperature to 1300^{o}C in air with a heating rate of 10^{o}C /min.

The formation of crystalline phases in the glass was investigated by isothermal heat treatment of the bulk samples for 10 hr to 100 hr at 850 ^{o}C in an electric furnace holding in air. Phase after the heat-treatment were identified from X-ray diffraction patterns, and the microstructures of the heat-treated sample were observed using scanning electron microscope (SEM, XL30, Philips Co., Holland). Qualitative composition analysis of various phases was carried out using X-ray energy dispersive spectroscopy (EDS, EDAX Co., Germany).

3.1.3 Bonding and Wetting Behavior

YSZ (8 mol% Y_2O_3-dope ZrO_2) was used as a substrate material for bonding and wetting test. The YSZ plates were prepared by colloidal filtration of the YSZ powder into pellet and sequentially sintering at 1600°C in air for 1 hr.

To examine the bonding characteristic and wetting behavior of the glass to YSZ plate, the glass bulk was put on YSZ plate and continuously heated up to 1100°C at a heating rate of 10°C/min in air. The contact angle is defined as the angle formed by two planes tangential to the liquid (or glass) and solid phase surfaces at the site of contact between the two phases. The change of contact angles at various temperatures was recorded.

3.1.4 Long-term operation stability

In order to investigate long-term stability when the cells operate, the G1A10 glass bulk was aging at the operation temperature, 650°C, and tested by XRD and TMA.

3.1.5 Interface reaction

To investigate the interface reaction between the glass/YSZ and glass/metallic interconnect (Crofer 22), the glass bulk placed on YSZ or Crofer 22 plates were first heated up to 1000°C at 10°C/min and held for 15 min to seal the glass and YSZ/Crofer 22 plates together, then the specimens were cooled down and aging at 650°C for a period of time. After the heat-treatment, the cross section of the specimens was examined using SEM to investigate microstructure change of the interface as a result of long-term treatment.

3.1.6 Bonding Strength

Bonding strength was measured from YSZ and Crofer 22 test bars with nominal depth, width and length of 5×5×20 mm^3 adhered by the selected paste, which was dispersed in H_2O with 1 wt % PVA. The YSZ to YSZ, Crofer 22 to Crofer 22, and YSZ to Crofer 22 adhered sample were tested at ambient temperature in air using the four-point flexure test method which is illustrated in Fig. 3.1, according to the recommendation in ASTM test standards C1161.[26,27] A displacement rate of 0.01 mm/s was applied in displacement control. A total of 3 test specimens were tested for each different sealing condition.

---

[26] C.A. Lewinsohn and S. Elangovan, in: Solid State Energy Conversion Alliance-Progress in Seals for Solid Oxide Fuel Cells (2003)

[27] ASTM C1161, annual Book of ASTM Standards, vol.1501, ASTM, West Conshohochen, PA, (2006)

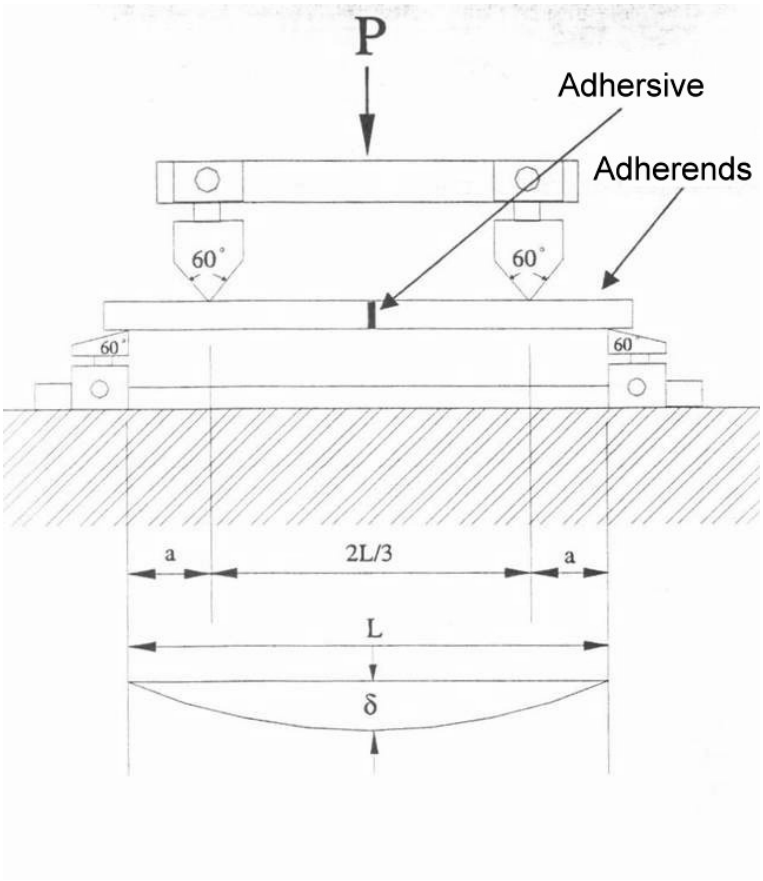

$$\sigma = \frac{3P(L-I)}{2Wt^2}$$

_	Flexural bending
S	Standard deviation
P	Tensile Strength
W	Specimen width
t	Specimen thickness

Fig. 3.1 Schematic of 4-point flexure test fixture.

3.2 Results

3.2.1 Thermal Properties of the Glasses

Fig. 3.2 shows the DTA patterns of five glasses and the thermal properties measured from DTA are also summarized in Table 3.1. Fig. 3.3 plots the T_g and T_c values as a function of composition. It indicates that with a higher B_2O_3/SiO_2 value, the glass-forming capability in this glass system would be changed, and this implies that the T_g and T_c of the glasses should meet the operation requirements. G1 glass shows better thermal properties among G0-G4 glasses. Moreover, with the addition of Al_2O_3, the crystallization of G0A5 and G1A10 could be retarded. The glass-forming ability and working temperature region would be increased.

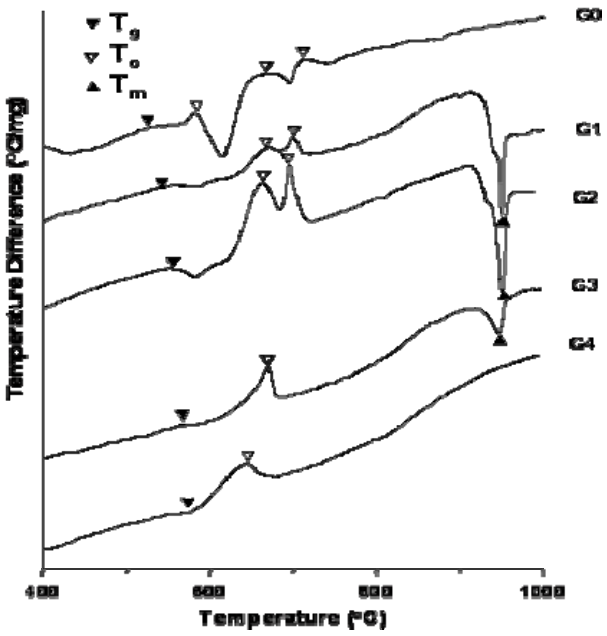

Fig. 3.2 DTA thermograms of G-series glass determined in air with a heating rate of 10°C/min from room temperature to 1000 °C

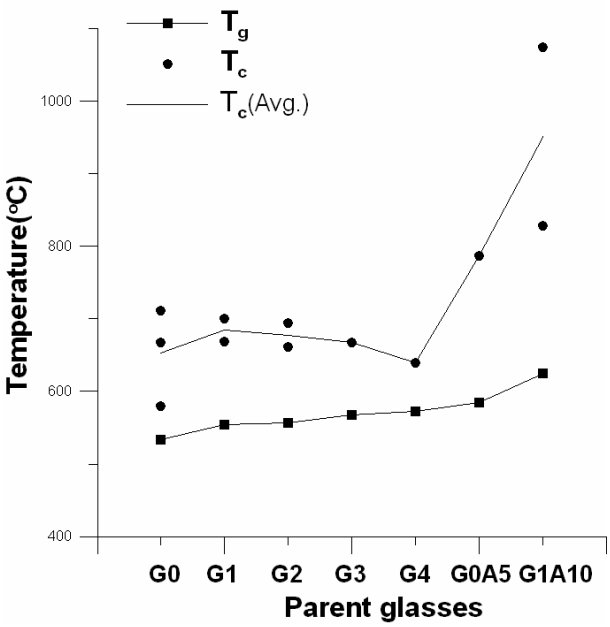

Fig. 3.3 Changes in T_g, T_c and T_m values of the G-series glass. The values were obtained from the DTA thermograms.

In general, the thermal stress developed at the sealed interface is strongly affected by the difference of CTE values between bonded materials and the T_g of the sealants. When fuel-cell stacks coolrf down to room temperature, stress begins to develop at the sealed interface only as the temperature decreases below the T_g of the sealants. This might cause severe damage to the stacks. Consequently, the T_g value of a compliant glass should be lower than the operation temperature capable of relaxing

the thermal stress produced at the interface. However, at the same time, the sealant must have adequate rigidity at the cell operating temperature so to prevent the sealant flowing out from the gap of the stacks to pollute the components. Therefore, for SOFCs designed to operate at 650-800^{o}C, a sealant with T_g lower or around 650^{o}C exhibits adequate rigidity at that temperature. Table 1 reveals that all the T_g of the glasses prepared meet to the compliant needs. Furthermore, the glass forming range of G1A10 is coincident with IT-SOFC operation temperature range (650-800^{o}C). Therefore, the latter analysis would be focused on the G1A10 glass.

3.2.2 Crystallization Behavior

X-ray diffraction patterns of the as-prepared glasses are shown in Fig. 3.4. Not all the as-quenched G-series glasses were found to be amorphous. But with the addition of Al_2O_3, the amorphous state of G0A5 and G1A10 would be retained.

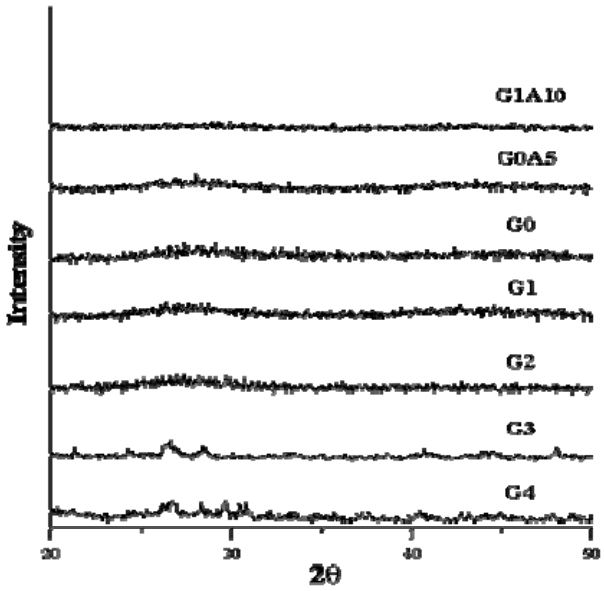

Fig. 3.4 XRD pattern of the as-prepared Ba-glasses.

In general, a glass-ceramics with a high degree of crystallization exhibits better mechanical properties than that of glass. Also, the glass-ceramics can have various CTE values depending on the types and volume fraction of crystalline phases in glass matrix. Glass-ceramics generally also show higher chemical stability than the glasses. Therefore, in present work of SOFC operation, the G1A10 glass was heat-treated at 850^{o}C to investigate the crystallization behavior.

Fig. 3.5 shows the X-ray patterns of G1A10 bulk glass heat-treated at 850^{o}C for 10 or 100 hr. The XRD pattern of the G0A5 bulk glass heat-treated for 10 hr at 850^{o}C

also plotted in Fig. 3.5.

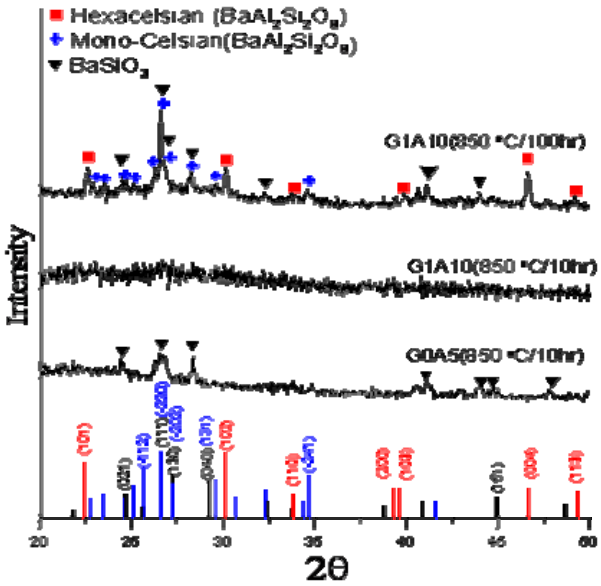

Fig. 3.5 XRD patterns of glasses heat-treated at 850°C for 10 and 100 hr to identify the crystalline phase.

For G1A10, according to the Gibbs' phase rule, four phases would be observed at equilibrium. Compareing the X-ray pattern with the SEM micrographs (Fig. 3.6) and EDS analysis, there existed three crystalline phases and one glass phase, which are hexacelsian ($BaAl_2Si_2O_8$), monocelsian ($BaAl_2Si_2O_8$), and barium silicates ($BaSiO_3$). Their CTE values of these crystalline phases are listed in Table 3.2. Hexacelsian always precipitates first, and is more compatible with the parent glasses than it's polymorph, monocelsian, in terms of CTE mismatch. According to this, the crystallization of hexacelsian is desirable for preparing a suitable sealant for SOFCs. But, the platy-like shape of the hexacelsian implies that the thermal expansion is not isotropic which would lead to cracking due to the hexacelsian crystals. In our detail observation, intergranular fractures along the hexacelsian happened and decreased the sealing strength. The fractures were also harmful to gas- tight ability of the seal.

Table 3.2 Crystalline phases and CTE value in G1A10[28]

[28] K. Scott Well, John E. Deibler, John S. Hardy, Dong Sang Kim, Guan Guang Xia, L.

Name	Composition	CTE (ppm)	Temperature Range (^{o}C)
Barium Silicates	$BaSiO_3$	12.5 9.4	20-550 20-1000
Hexacelsian	$BaAl_2Si_2O_8$	8.0	20-1000
Monocelsian	$BaAl_2Si_2O_8$	2.7	20-1000

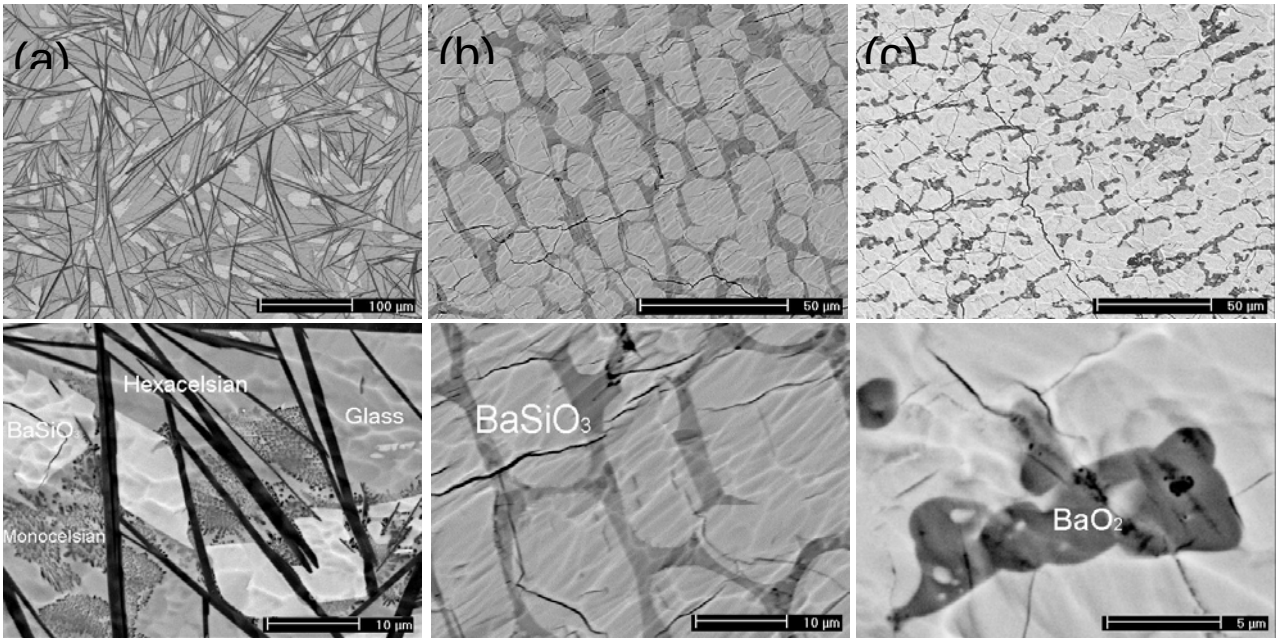

Fig. 3.6 SEM micrographs imaged by backscattering of (a)G1A10 heat treated for 100 hr, (b)G0A5 heat treated for 10hr, and (c)G0 heat-treated for 10 hr at 850^{o}C to identify the crystalline phases.

3.2.3 Wetting Behavior of Glasses

Wetting behavior is an important factor that has to take into consideration for

---

A. Chick, and Chris A. Coyle, "Rupture Testing as a Tool for Developing Planar Solid Oxide Fuel Cell Seals, " J. Mater. Sci. Perm., 13, 316-326 (2004)

preparing a reliable glass sealant. Since the shape change of glass occurs because of decreasing of the viscosity., which is a function of temperature. According to Table 3.1, G1A10 glass shows a higher T_g value than that of G0 and G0A5 glasses. Fig. 3.7 shows the shape change of three glass bulks: G0, G0A5, and G1A10, placed on the YSZ plate at heating rate of 10°C/min. G0 and G05A glasses with a higher B_2O_3/SiO_2 ratio and lower Al_2O_3 additive, started wetting at 1050 °C and 1000 °C, but G1A10 started wetting at 800°C. This is because of a crystalline phase growing in G0 and G0A5 at 580°C, which would result in a higher wetting temperature and viscosity.

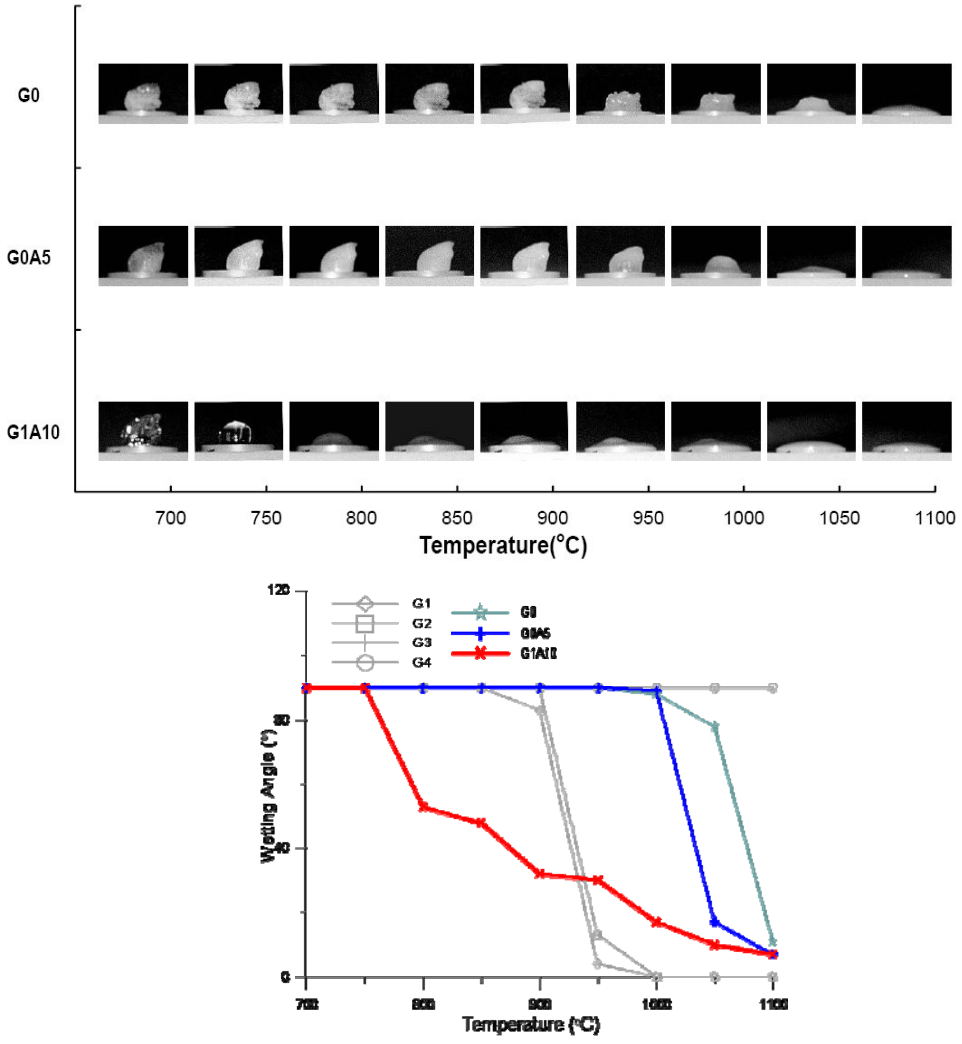

Fig. 3.7 (a) Shape change of G0,G0A5, and G1A10 glass bulk placed on the YSZ plate with increasing temperature (heating rate of 10°C/min),(b)Contact angle measurements of various glass bulks placed on the YSZ plate with increasing temperature (heating rate of 10°C/min)

Fig. 3.8 shows the more detailed shape change behavior of the G1A10 bulks placed on a YSZ plate with a heating rate of 10°C/min. G1A10 glass is the better sealing material than the others. From the observation, 970°C was the suitable

sealing temperature.

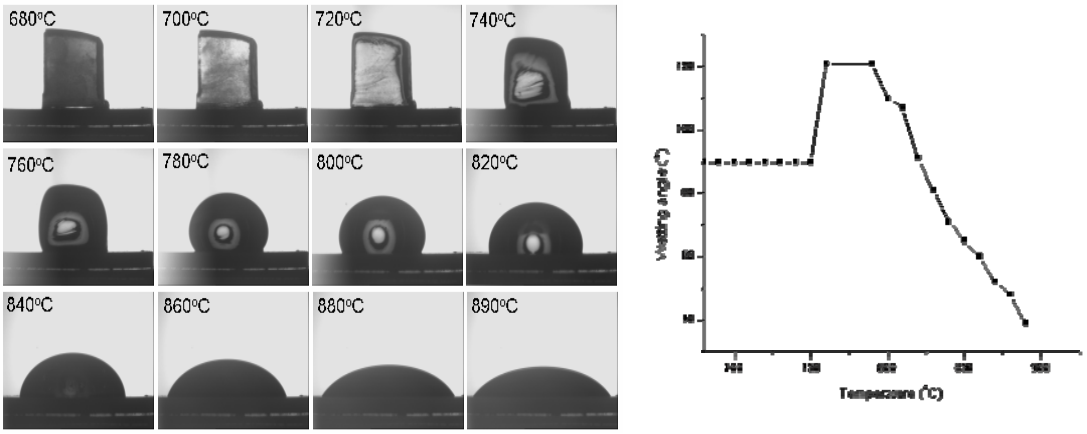

Fig. 3.8 (a) More detailed shape change and (b) Contact angle measurements of G1A10 glass bulk placed on the YSZ plate with increasing temperature (heating rate of 10°C/min)

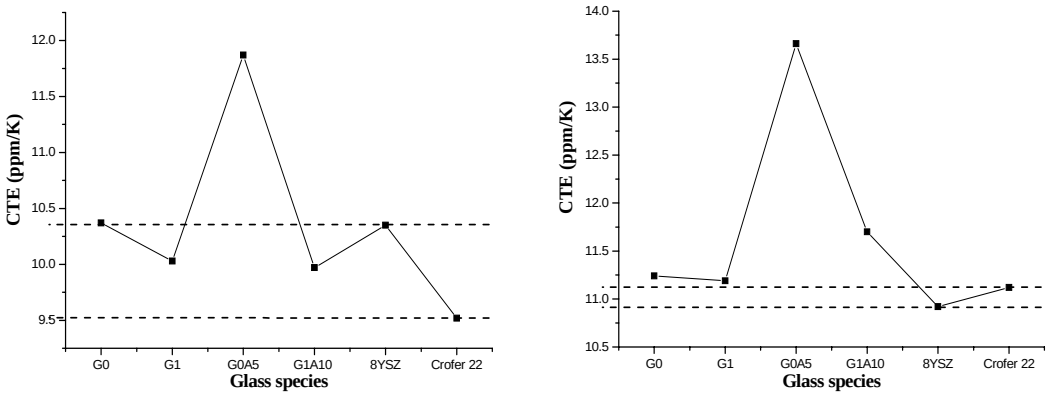

Fig. 3.9 CTE value of G0, G1, G0A5, G1A10 glass, YSZ, and Crofer 22 when (a) with heating rate of 10°C/min to 600°C and (b) with air cooling from 600°C to room temperature.

3.2.4 Long-term Stability Analysis

Fig. 3.9 plots the CTE value of some glass sealants, and also the YSZ and Crofer 22. When tested in heating cycle, the CTE value of G0A5 is too high to meet that of YSZ, and the other glass sealants, G0, G1, and G1A10, are in the range (9.5-10.4x10^{-6}/K) between YSZ an Crofer 22. When tested in cooling cycle, only the CTE of G0, G1A10, and G1 glasses are very close (less than 1.0 ppm/K difference) to that of YSZ and Crofer 22.

Fig. 3.10(a) shows the XRD pattern of the G1A10 glass aging at 650°C for 10 to 30 hr. No crystalline precipitates were detected. Fig. 10(b) shows the change of the CTE value of G1A10 aging at 650°C for 10 to 30 hr. As the heat-treatment extended, the CTE value kept in the range of 10 to 13.5 ppm/K. The accuracy of the data is poor, needs more work on this.

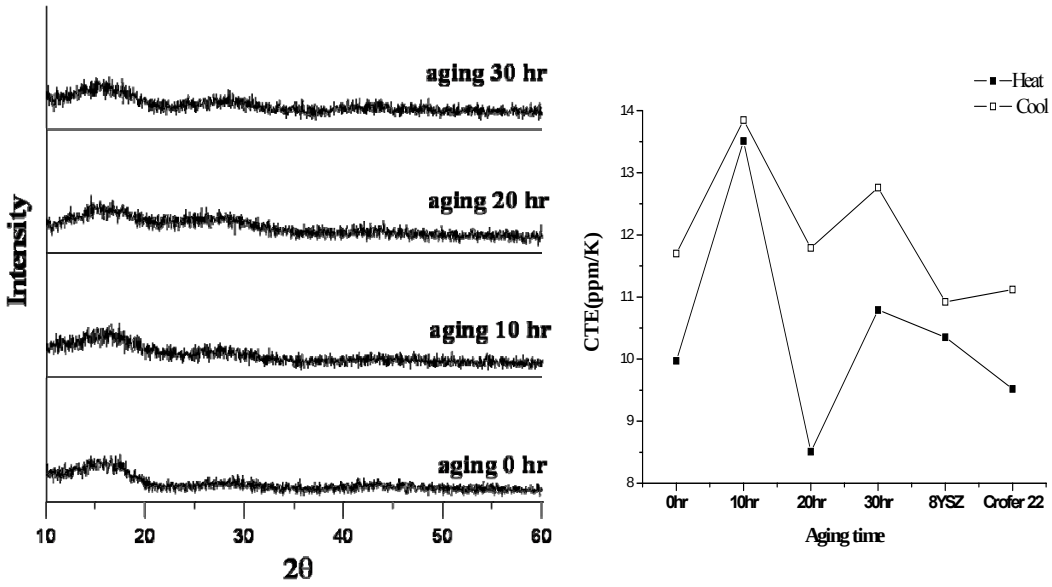

Fig. 3.10 (a)XRD patterns, and (b) the CTE value of G1A10 glass aging at 650°C for 10 to 30 hr.

3.2.5 Interface reaction between glass and YSZ/Crofer 22

Fig. 3.11 shows the microstructure of the G1A10/ YSZ sealing interface which were heat-treated at 650°C for 10-30 hr after being bonded at 970°C for 15 min. It was apparent that a reaction layer found in the glass next to the sealing interface. Fig. 3.12 shows the microstructure of the G1A10/ Crofer 22 sealing interface which were heat-treated at 650°C for 10 or 50 hr after being bonded at 970°C for 15 min. There also existed a reaction layer at the sealing interface of G1A10/ Crofer 22. Small cracks were found along the plate-shape crystalline phase and the residual glass phase.

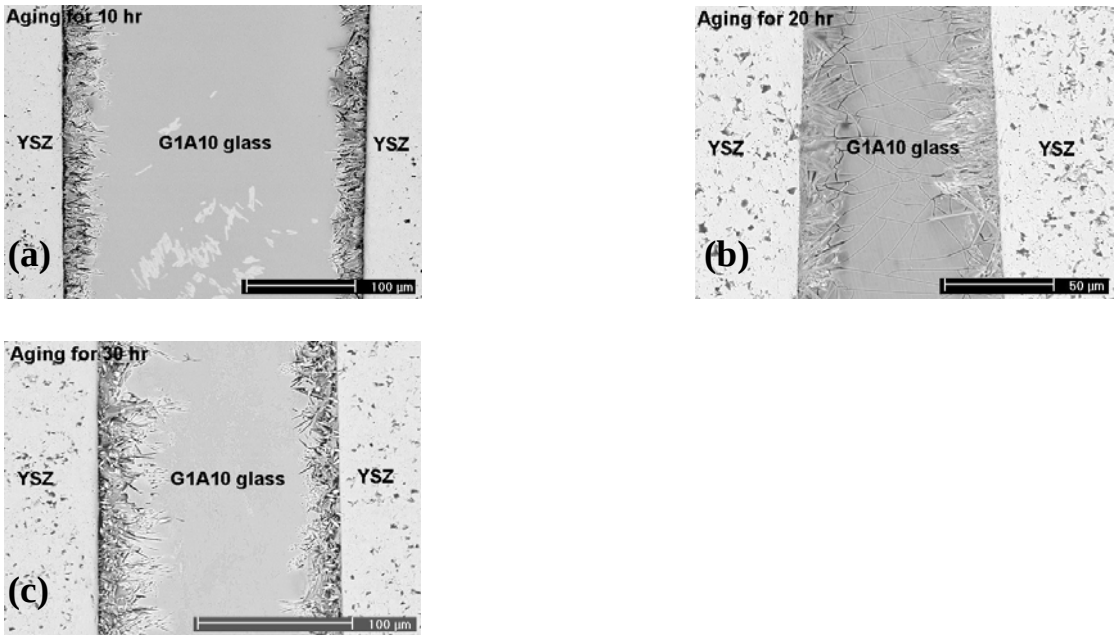

Fig. 3.11 SEM micrographs imaged by backscattering of G1A10 (a)aging for 10 hr, (b) aging for 20 hr, and (c) aging for 30 hr at 650°C.

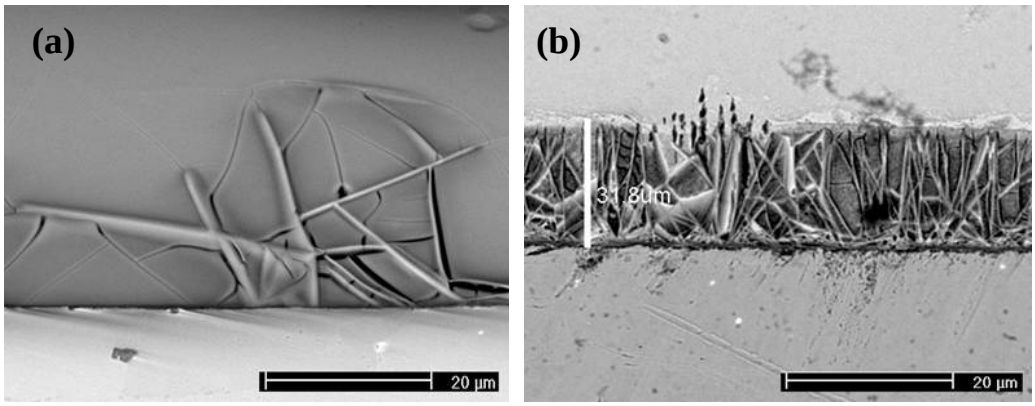

Fig. 3.12 SEM micrographs imaged by backscattering of G1A10/Crofer 22 aging for (a) 10hr and (b) for 50 hr after sealing at 950°C for 10min.

3.2.6 Bonding Strength

Results of bonding strength testing were shown in Table 3.3 The strength of the as sealed sample (10-12 MPa) is still too low to withstand the thermal stress during operation. Observing the morphology of the fractured sample, there existed lots of gas pores within the glass, and leading to low bonding strength.

From the fracture morphology of the adhered samples, there existed lots of gas pores and leading to low bonding strength. In order to decrease the amounts of the pores, using the glass tape instead of brushing the glass paste to seal the sample would

be a good resolution.

Table 3.3 Bonding strength results of the test specimens as sealed at 970°C and heat-treated at 650°C

	YSZ to YSZ as sealed at 970°C	Crofer 22 to Crofer 22 as sealed at 970°C	YSZ to Crofer 22 as sealed at 970°C	YSZ to Crofer 22 970°C aging for 5 hr
Flexure strength (MPa)	10.88	10.08	12.4	9.66

IV. Leakage Rate Measurement of Glass G1A10

Another important characteristic of these sealing glass systems is the leakage rate as it is used to seal the gaps between SOFC components. It determines whether the SOFC is reliable or not for short or long-term applications. This subject includes two parts which are shown below:

- Leakage test device designing
- Leakage rate measurement

4.1 Design of Leakage Test Device

The equipment is totally made by S420 stainless steel in the causes of good oxidization resistance and good coefficient of thermal expansion (CTE) matching with 8YSZ, glass sealant and interconnect (Crofer 22APU). Fig. 4.1 shows the AutoCAD diagram of the device, and the assembly diagram is also shown in Fig. 4.2.

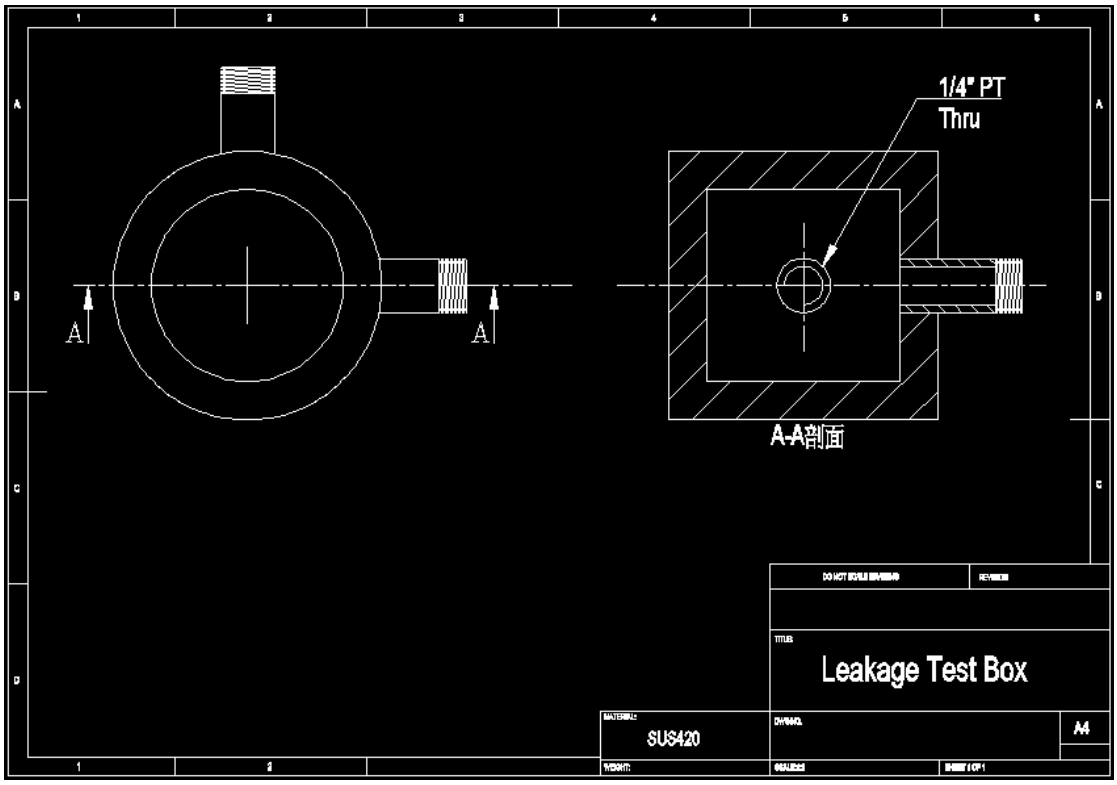

Fig. 4.1 AutoCAD diagram of the leakage test device.

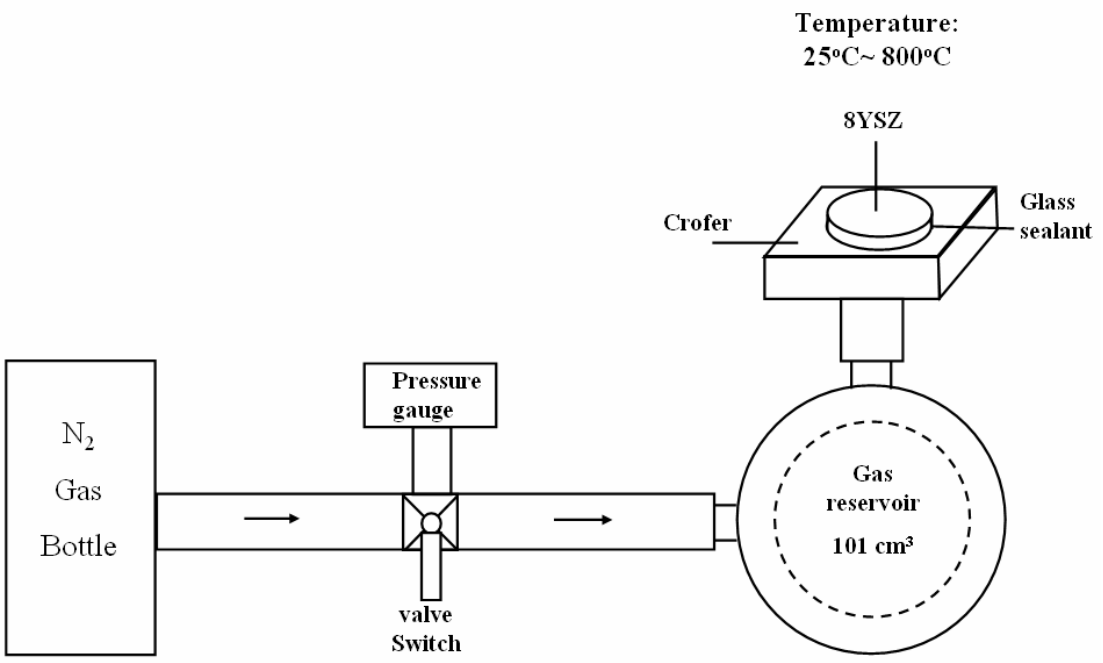

Fig. 4.2 Assembly diagram of leakage test device.

4.2 Leakage Rate Measurement

We have completed the leakage test of the G1A10 glass at the temperatures at 25°C and 600°C. The leakage rate is calculated by the following equation [29]:

$$L = \frac{(P_i - P_f)V}{P_f \Delta t C}(sccc/cm) \quad \text{.....(4.1)}$$

Where L is the leakage rate, P_i is the initial pressure, P_f is the final pressure, V is the volume of the gas reservoir, $\triangle$t is the time elapsed as the pressure decreases from Pi to P_f, and C is the circumferential length of the sealant.

According to the latest literature review [30,31,32,33], most of leakage tests are operated below 0.2 bar for the sake of being closer to the operating pressure of a SOFC.

4.2.1 Test Sample Preparation

The test samples included a piece of disk-shaped 8YSZ, a piece of Crofer 22 and

---

[29] S. Le, K. Sun, N. Zhang, Y. Shao, M. An, Q. Fu, X. Zhu, *J. Power Sources*, 168 (2007) 447–452

[30] Y.-S. Chou, J. W. Stevenson , R. N. Gow, *J. Power Sources*, *170 (2007) 395–400.*

[31] Y.-S. Chou*, J. W. Stevenson, J. *Power Sources,* 135 (2004) 72–78

[32] R. Wang, Z. L¨u, C. Liu, R. Zhu, X. Huang, B. Wei, N. Ai, W. Su, *J. Alloys and Compounds*, 432 (2007) 189–193

[33] SECA, Website (*http://www.netl.doe.gov/*)

5 ml of G1A10 glass paste. Disk-shaped 8YSZ has been sintered at 1500^{o}C to full density and had the diameter of 15.1 mm. The G1A10 glass paste consists of 2.2 g G1A10 glass powder, whose mean particle size was 10 μm, and 2.2 g 99.5% ethanol. Crofer 22 was cut into the size of 2×2×2 cm^{3}, with an additional hole (5 mm in diameter) at the center.

4.2.2 Flow Chart of Joint

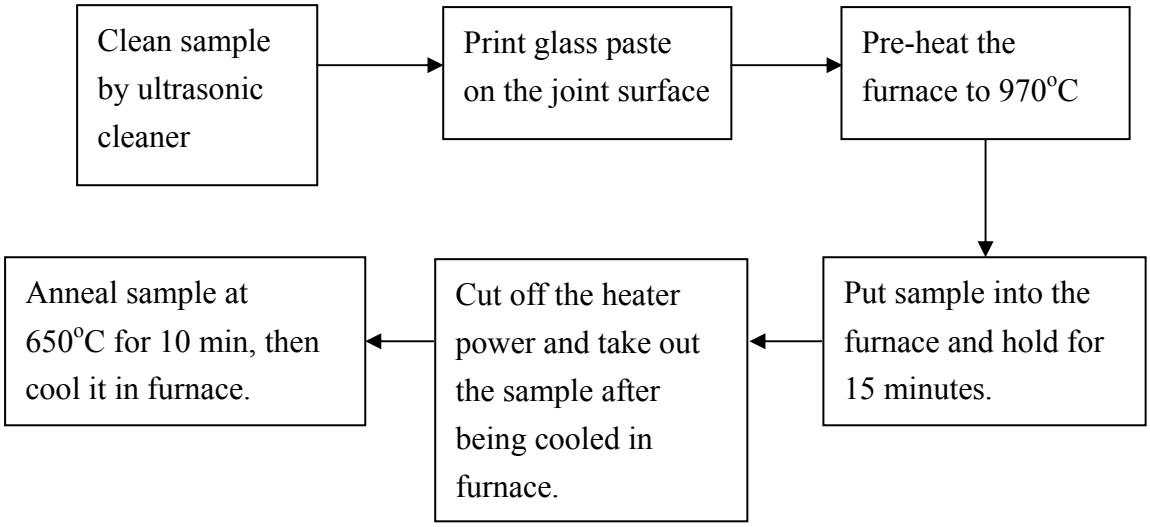

4.3 Results

The leakage rate of G1A10 glass sealant at ambient temperature is shown in the Fig.4.3.

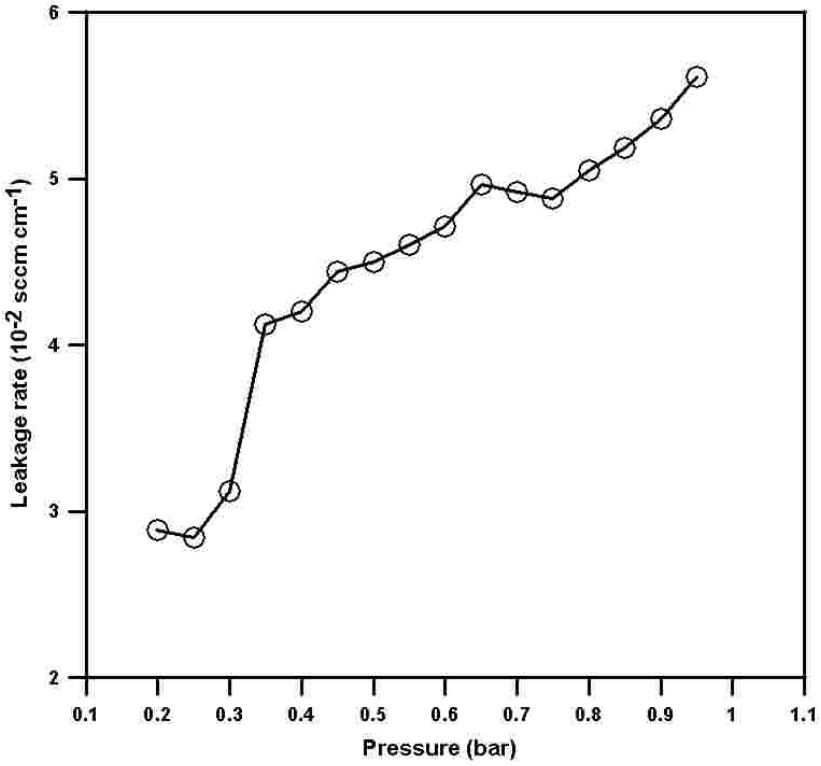

Fig. 4.3 The leakage rate at room temperature

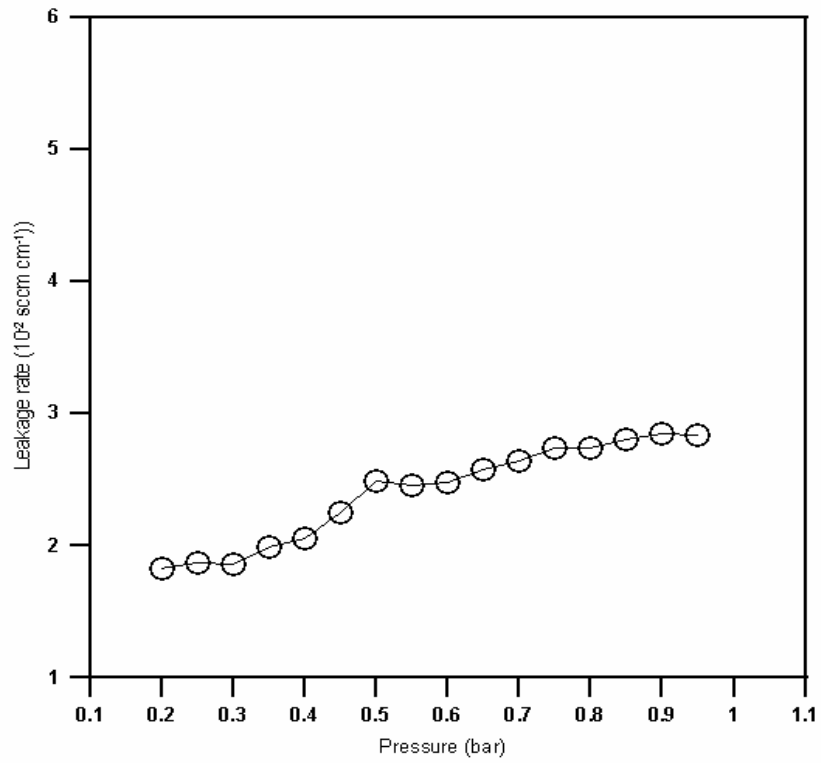

Fig. 4.4 The leakage rate at 600^{o}C

The leakage rate of glass sealant is tested with pure nitrogen gas at different over-pressures, and the system has a background leakage of 3.0×10^{-4} sccm cm^{-1}. The

room temperature test result is shown in Fig 4.3. The leakage rate has the lowest value (0.03 sccm cm^{-1}) at the over-pressure below 0.25 bar and the highest value (0.06 sccm cm^{-1}) at the pressure of 1.0 bar,

The leakage rate at 600^{o}C is shown in Fig 4.4. Surprisingly, the leakage rate at 600^{o}C is between 0.028 sccm cm^{-1} and 0.018 sccm cm^{-1} which is better than that at room temperature. And the leakage rate at 600^{o}C shows high consistency at different over-pressures.

According to the literatures, the best leakage rate result of glass-ceramic sealant is 5 $\times 10^{-6}$ sccm cm^{-1} [4], while the compressive sealant has the best record of 5 $\times 10^{-4}$ sccm cm^{-1} [3]. Apparently, we need much more efforts on the development of better sealing glass. But in the view of engineering aspect, a fuel leakage percentage of 0.6% is acceptable for SOFC sealing requirement [1]. In the case of our self-manufactured SOFC equipment, which has a sealing length of 34 cm, the maximum fuel lose will be 0.95 sccm at 600^{o}C and a over-pressure less than 1.0 bar. If we set the fuel flow rate at 500 sccm then the fuel loss will be only 0.19%.

V. Conclusions

Bi_2O_3-ZnO-SiO_2-B_2O_3 glass system shows a good wetting on sintered YSZ plate. Bi_2O_3 diffused slightly into YSZ along the grain boundary at 650°C and the Bi-species did not apparently react with YSZ. Zn_2SiO_4 segregated at the interface next to YSZ to form a barrier layer and prevent Bi_2O_3 diffusion. The crystallization and Bi diffusion can enhance the bonding strength in joining to YSZ, but not to Kovar. Bi-oxide based glass reacted with Kovar seriously and caused a weak interface.

A significant creeping behavior of B4 and P1 glass ceramics was observed, which might perform a self-healing of cracks. Viscosity of residual glass was calculated in the range of 10^5 Pa*s. B4-glass has several advantages such as good wetting behavior, easy formation, better creep behavior and suitable T_g as an SOFC sealant better than lead-glass system. The disadvantage of B4-glass is low CTE value which decreases with crystallization. A 10-30 wt% ZrO_2-dopant could increase the CTE of glass-ceramic and prevent cracks formation. Table 4.1 summarizes the differences of P1 and B4 glasses.

The glass-ceramics sealants based on BaO-SiO_2-B_2O_3 with Al_2O_3 addition have been developed to meet the requirements for planar solid-oxide fuel cells. The thermal properties of the G-series glasses and the wetting behavior revealed that the glass forming range and the fluidity of the glass were strongly influenced by the B_2O_3/SiO_2 ratio. Also the crystallization can be retarded by addition of Al_2O_3. For the concerns, G1A10 glass is the most probable sealant for planer SOFC operating at 650-800°C.

Three main crystalline phases in G1 glass would precipitate along the interface of YSZ/amorphous glass matrix, including $BaSiO_3$, monocelsian, and hexacelsian. Hexacelsian has a CTE value of about 8 ppm/K which is more compatible with YSZ than monocelsian, which has a CTE value of 2.7 ppm/K. Because of the plate-liked shape of the hexacelsian grains, its CTE value is not isotropic. Therefore, the change of preventing the formation of monocelsian phase and shortening the aspect ratio of hexacelsian grain are the important issues in future work.

From the cross-sectional morphologies of the glass sealing with YSZ or Crofer 22, there existed a crystalline layer at the interface. The interfacial phase may lead to a thermal expansion mismatch and induce thermal stresses. Not only fine cracks were formed along and inside the crystalline phase, but also a gap was formed between the parent glass and the reaction layer. This would degrade the long-term stability of the sealants.

G1A10 glass is a kind of good sealant for SOFC, which is demonstrated having a acceptable leakage rate for the common SOFC which is operated at the over-pressure lower than 1.0 bar. But the higher the operating pressure is, the higher the efficiency of the SOFC will be.

Table 5.1 Comparisons of no. P1 glass and B4-glass.

Parameters	P1-glass	B4-glass
Basic material properties		
Composition	with lead	lead-free
Porosity of open-pore after 650°C 10 hr	67%	87%
Ratio of B_2O_3/SiO_2 in formulation	2.15	0.25
Thermal properties		
Glass transition temperature (T_g)	360°C	450°C
Melting point (T_m)	600°C	900°C
CTE of glass	9.1 ppm/K	11.9 ppm/K
CTE after 650°C 10 hr (quenched)	9.1 ppm/K	4.1 ppm/K
Crystalline phases		
Crystalline phases at 650°C	4 kinds	4 kinds
Interfacial properties		
Interface reaction	Significant, $PbZrO_3$ phase	Unobvious, only reacted with impurity at grain boundary
Diffusion profile after 650°C for 10 hr	20 μm	15 μm
Interface attacked at 650°C for 10 hr	Seriously	Slightly
Diffusion path	lattice and grain boundary	Via. grain boundary
Self-barrier formation	No	Yes, Zn_2SiO_4
Electrical Conductivity		
Electrical conductivity at 600°C	-	1.6×10^{-3} S/m

VI. 計畫成果自評

兩年的研究工作共合成兩個系列的玻璃陶瓷材料，並與一鉛系列的低溫玻璃相比較。除原使用之金屬(不鏽鋼及 Kovar)因抗氧化性不佳，改爲 Crofer 22，其他規劃之工作項目及目標均符合原計畫內容。

原研究內容規劃三個主題，第一是合成低熔點玻璃，用於固性封裝或柔性封裝，量測並報導兩種玻璃之性質，包括軟化點、潤濕性、電絕緣性等。第二是分析探討不同材料與封裝玻璃之界面反應現象。第三主題是探討玻璃系統的封裝特性，我們將在室溫及高操作溫度下，將不同材料疊層之組合進行氣體洩漏率及玻璃強度之測試。相關的界面反應動力及分子擴散機制也予以深入探討。

研究成果已整理出兩篇論文，一篇玻璃陶瓷材料方面之專利，前者將投稿國際型期刊，後者將伸請國內及國外專利。此外，後續仍有相關之主題值得繼續進行(見 96 年度研究計畫)。

赴德國研究報告

The Report of Investigation in Germany

主題：固態氧化物燃料電池之封裝玻璃選擇、特性分析與高溫潛變之研究

The Study of Material Selection, Characters Analysis and High temperature Creeping Behavior of Sealing Glass for SOFC

報告人：陳右儒

指導教授：韋文誠 教授 and Andreas Roosen 教授

研究地點：Friedrich-Alexander-University, Erlangen- Nurnberg

研究時間：2006.08.01~2006.09.23

Abstract

The investigation at Friedrich-Alexander-University, Erlangen-Nurmberg focused on the sealing material selection, creep behavior, viscosity variation and the composition analysis. Treated samples with different heat treatment conditions, and discussing the variation of glass phase content to creep behavior. There are some problems in G1 serial glass which was reported. In this investigation also tried to adjust the composition to modify the system to reach suitable sealing properties for SOFC.

I. **Introduction**

Glass is the most suitable material as a sealant for SOFC. There are several requirements in mechanical, chemical and electrical aspects for the selection of a suitable glass sealant. Three properties are very fundamentals for the glass. One is the glass transition temperature (T_g) and the other is the coefficient of thermal expansion (CTE) of the glass-ceramics. The glass transition temperature is important to allow flowing to maintain gas tight. The coefficient of thermal expansion (CTE) must match other cell components, such as the yttria-stabilized zirconia (YSZ) electrolyte and the interconnect material, to minimize thermal stresses. Finally, the electric resistivity of the glass-ceramics should better be than 10^6 ohm/cm.

Sealing glasses are categorized to two classes. One is compliant glass; the other is rigid glass. Previous one has the T_g (glass transition temperature) lower than the service temperature (T_s), therefore, shows slightly creeping at the service temperature. The rigid glass can not creep; therefore, it should have a full match of thermal expansion coefficient (CTE) with the solid electrolyte. The glass in this study will only develop the compliant glass due to the technical consideration on the CTE.

Viscosity is one of the important properties of a glass-ceramics. Creeping and interfacial reactions are also two major causes for the degradation of sealing glass at service temperature. The property is depending on temperature and compositional, especially at temperature above glass transition temperature [Rawson, 1980]. It was reported that glass can be deformed by external pressure above the glass transition temperature, which is more time-dependent [Koide et al., 1996]. Beside interactive time and temperature, inclusions and degree of crystallization are also affected the viscosity of a glass [Heymann *et al*., 1995].

After measuring the viscosity of glass, it is possible to predict crystallization tendency and the creep behavior of glass. So the purpose of this experiment to Germany is to measure the viscosity of three glass-ceramics systems, Bi-Zn-B-Si oxide glass, Ba-B-Si oxide glass, and Ba-Si-B-La oxide glass, so to understand how the crystallization affects the rheology of glass. So there are four main tasks listed below.

- Investigate the relationship of rheological properties as a function of glass fraction:

  1. Preparing B4, G1, and G1 (+La_2O_3) Glasses;

2. Analyze the rheology (creep behavior) of the samples with different glass fractions;
3. Measure the fraction of residual glass phase in annealed samples from SEM micrographs.

- Analyze the glass composition by ICP.
- Determine the coefficient of thermal expansion of glasses (B4, G1 and G1+La).
- Conduct one High temperature XRD (B4 10 hr).

2. Experimental procedure

Fig. 1 shows the experiential procedure flow chart. We have four kinds of glass systems in this investigation listed in Table 1.

Table 1 Glass composition and thermal properties in this investigation.

	Composition	T_g (^oC)	T_m (^oC)
G1	$50BaO\text{-}22B_2O_3\text{-}28SiO_2$	550	950
G1-5I	$50BaO\text{-}22B_2O_3\text{-}28SiO_2\text{-}5La_2O_3$	560	890
G1-10	$50BaO\text{-}22B_2O_3\text{-}28SiO_2\text{-}10Al_2O_3$	650	1200
B4	$30Bi_2O_3\text{-}20ZnO\text{-}10B_2O_3\text{-}40SiO_2$	450	930

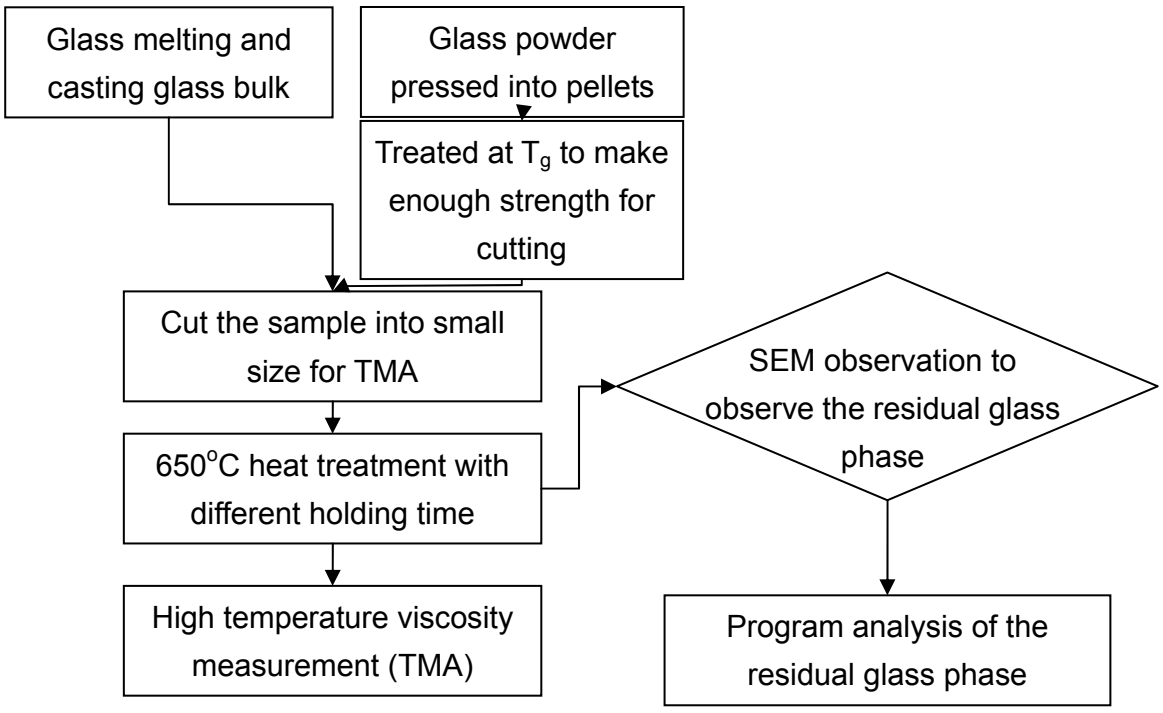

Fig. 1. The flow chart of experimental procedure in this investigation.

The first step in this investigation is glass casting. Because porosity will affect the creep behavior and thermal expansion coefficient, it is better to use a dense sample for analysis. An SEM was employed to observe the microstructure of these casting samples. The second step is wetting behavior measurement. A glass with a good wetting on YSZ sintered plate is needed.

It is easy to measure the residual glass phase by computer program. Image-C is a kind of microstructure analysis program. Using this program the can calculate the residual glass phase in SEM image. In this part, each condition was calculated by 15 pictures and gets an average value.

The fourth part is the most important part in this investigation. Three types of samples were employed for creep investigation list below.

- Casting glass bulk, it is a dense glass bulk without porosity. We made these samples by glass casting into graphite mold with air and annealing at 300^{o}C for 1 hr.
- Using sandwich sample (YSZ/glass/YSZ) for investigation. These samples were made by painting glass paste between two YSZ sintered bulks, and melt the glass at its melting temperature for 15 min then quenched in the air. The paste was made from glass powder and de-ionized water with 1wt% PVB.

After measuring the creep behavior with different loading by TMA, the data can be analyzed by two models so to calculate the apparent viscosity (the viscosity included crystals). We will discusse in next chapter.

Samples for coefficient of thermal expansion measurement, ICP (Inductively Coupled Plasma) compositional analysis, and high temperature XRD were prepared in Taiwan and analyzed at Erlangen.

3. Theory and theoretical models

The shear viscosity is most defined in terms of the flow situation shown in Fig. 2. There are several kinds of methods to measure the viscosity of glass. In this investigation, a parallel plate method was employed.

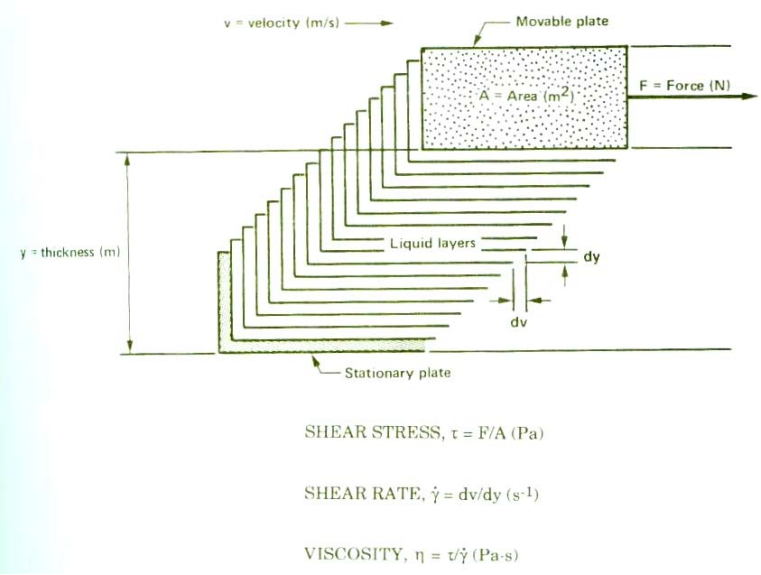

Fig. 2. Model indicating viscous flow and definitions of shear stress, shear rate, and coefficient of viscosity [Reed, 1995].

There are two kinds of model to calculate the viscosity. One is just for high content glass material. It uses a circular disc of glass, which is sandwiched between two refectory ceramic plates. The change in distance between the plates when a force is applied. Viscosity of corresponding glass, η, are calculated from the measured strain rate according to the formula [Kumar *et al*., 2005]

$$\eta = \frac{\sigma}{2(1+\upsilon)\dot{\varepsilon}} = \frac{\sigma}{3\dot{\varepsilon}} \quad \text{.....(1)}$$

where σ is the applied stress. The unit of σ is Pa. $\dot{\varepsilon}$ is the minimum strain rate measured during creep tests and υ is the Poisson's ratio of glass bulk. The viscosity range in 10^4-10^8 Pa・s can be measured by this parallel plate method [Rawson, 1980].

In general, viscosity is affected by temperature. The temperature dependency of viscosity can be described and calculated by Arrhenius equation [Rawson, 1980]:

$$\eta(T) = \exp(\frac{E_\eta}{RT}) \quad \text{.....(2)}$$

The degree of crystallization in the glass also affects the viscosity. It changes with the amount, size, shape of crystals, which has been described as below [Boccaccini, 1998 & Kumar *et al*., 2005]:

$$\eta = \eta_0 (1 - f)^m \quad \text{.....(3)}$$

$$m = \frac{3F - 2}{3F(1 - 2F)} \quad \text{.....(4)}$$

Where η_0 is the viscosity of the glass, f is the volume fraction of the crystals (inclusions) and m is constant, a function of the shape of crystals. F is the shape factor.

The other method is suit for ceramic system (less content of glass). In this condition, Maxwell element descriptions (both elastic and viscous behavior) shown in Fig. 3 will be more suitable to calculate the viscosity. It can be imagined that there are spring and viscose in the bulk [Cai *et al.* (1997)].

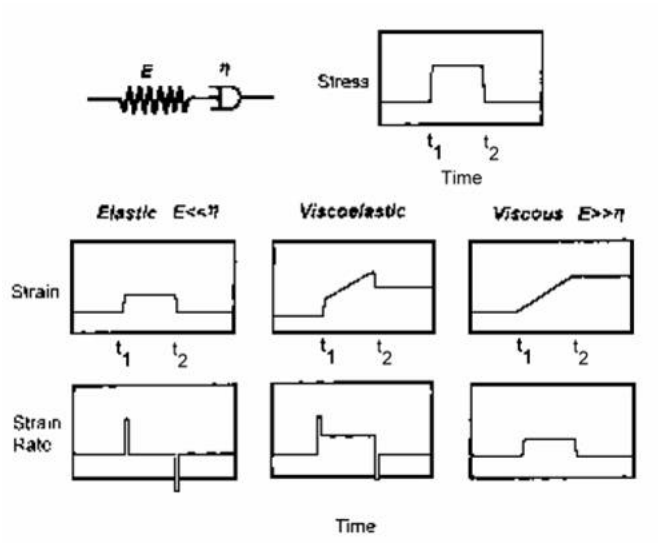

Fig. 3. The schematic diagram of Maxwell element

Equation shows below is the general solution of Maxwell element.

$$\varepsilon(t) = \frac{\sigma_0}{E} + \frac{\sigma_0}{\eta} t \quad \text{.....(5)}$$

Differentiating the ε(t) expression in above equation with respect to time, one obtains

$$\eta = \frac{\sigma_0}{\dot{\varepsilon}} \quad \dot{\varepsilon} = \dot{\varepsilon}_1 - \dot{\varepsilon}_f \quad \text{.....(6)}$$

ε_l is the strain rate under the load and ε_f is the strain rate without the load. Then we can get the viscosity value. So select different loading interval at specific temperature. We get a

viscosity vs. temperature relation diagram.

4. Results and discussion

The results of G1 system

Casting G1 glass is hard to get a pure glass (without crystallization). Fig. 4-(a) shows the microstructure of as-cast G1 glass. There are a large amount of crystals inside. This might be caused by a rapidly crystallization during glass casting. Fig. 4-(b) shows the lower magnification of as-cast G1 glass. The formation of cracks is due to low strength and is hard to made TMA sample. Both of conditions with annealing at 300^{o}C and without, G1 glass still show a rapidly crystallization.

Fig. 5 shows the wetting behavior of G1-cast glass. The melting point of G1 glass is 950^{o}C, but there is no wetting behavior for the glass-ceramics. Casting method can't form a pure glass for SOFC application. The residual glass in Fig. 4-(a) is less than 1.5% measured by Image-C program.

Sandwich sample of YSZ/G1/YSZ also have the same problem. Rapidly crystallization was observed in Fig. 6 and Fig. 7. After holding at 650^{o}C for 10 min (Fig. 6) and 1 hr (Fig. 7), the state of crystallization have no significant change. The average size of these crystals is 21 μm, and the thickness of glass-ceramic layer is 100 μm.

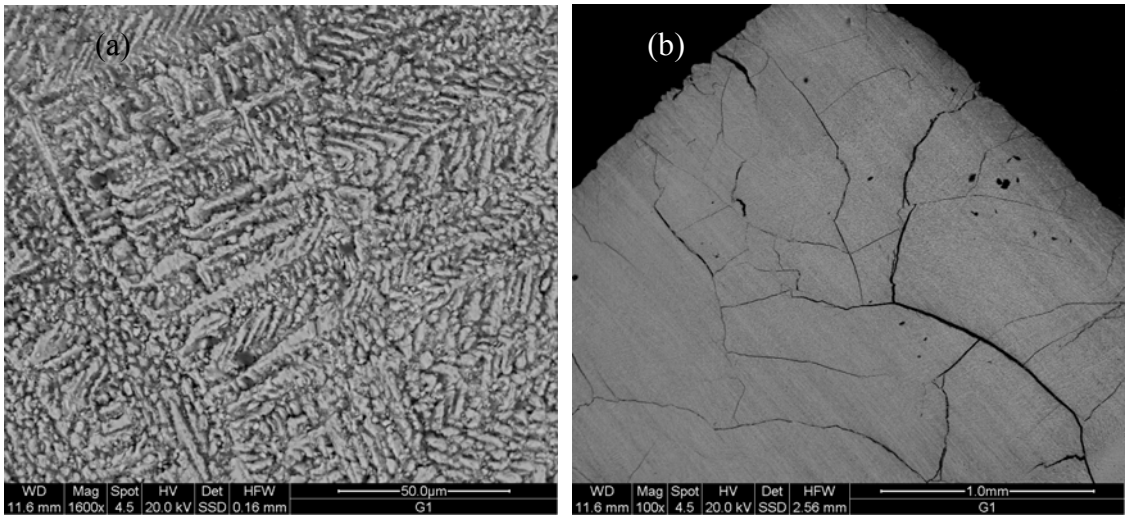

Fig. 4. (a) The microstructure of as-cast G1 glass. It shows a large amount of crystals in the bulk. (b) The lower magnification image of as-cast G1 glass.

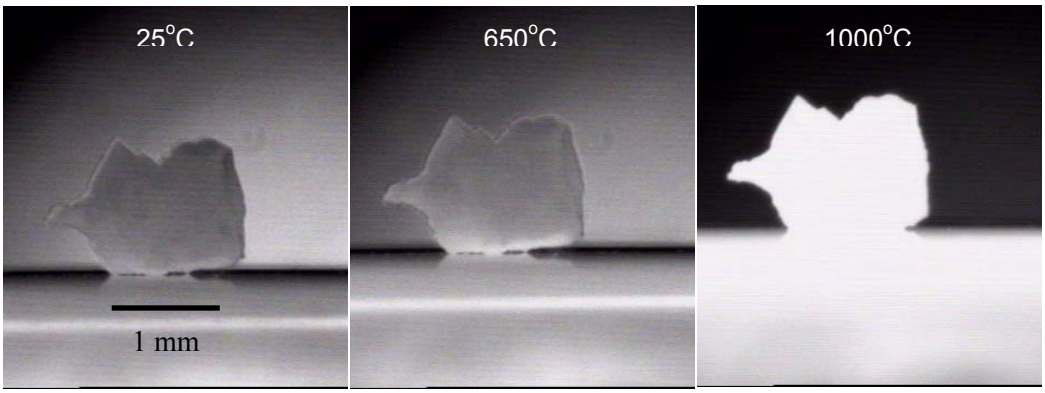

Fig. 5. The wetting behavior of as-cast G1 glass at different temperature. There is no wetting behavior for this glass-ceramic.

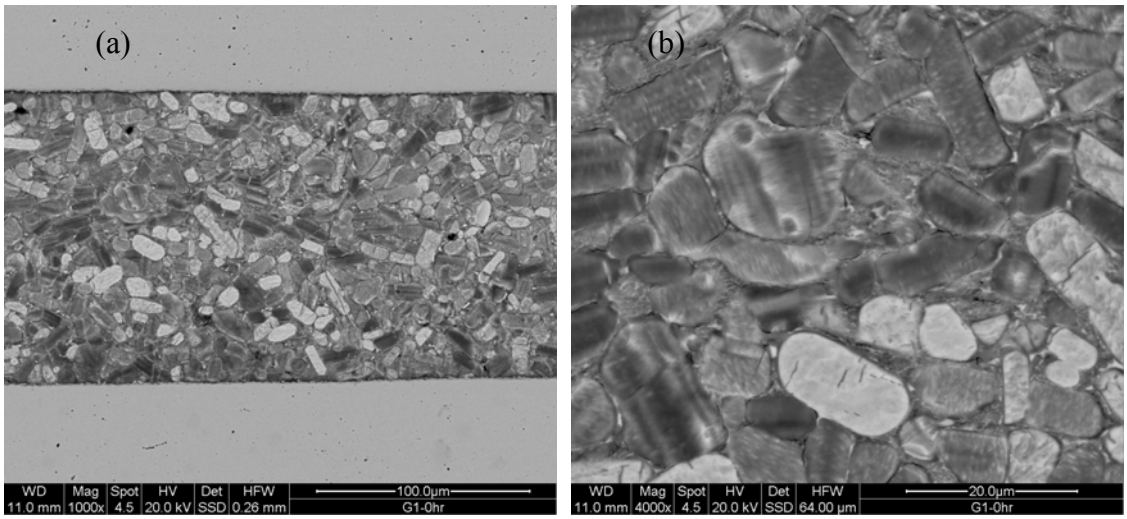

Fig. 6. The cross-section micrograph of sandwich sample YSZ/G1/YSZ after 650°C 10 min heat-treatment.

The results of G1-5L glass

In this system, there is inhomogeneous crystallization in G1-5L as-cast glass shown in Fig. 8. The 5 mol% La_2O_3 doped will affect the crystallization behavior and decrease the viscosity of glass. The reason may be caused by different cooling rate. This glass caused some problems as a sealing material. This inhomogeneous crystallization might happen during the glass paste (powder) melting, wetting on component and cooling. So this system we discuss less in this investigation.

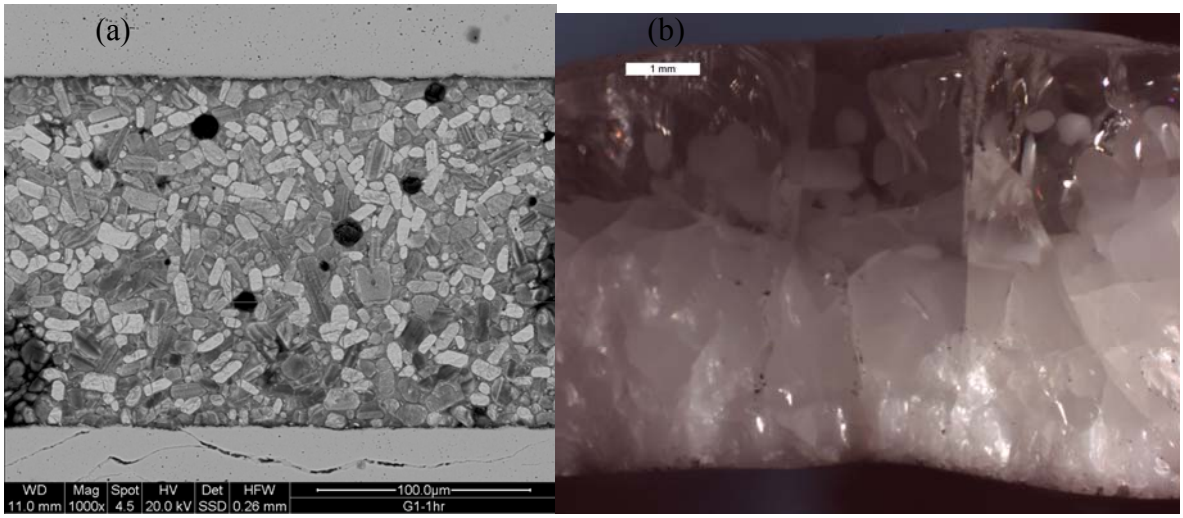

Fig. 7. The cross-section micrograph of sandwich sample YSZ/G1/YSZ after 650^{o}C 1 hr heat-treatment.

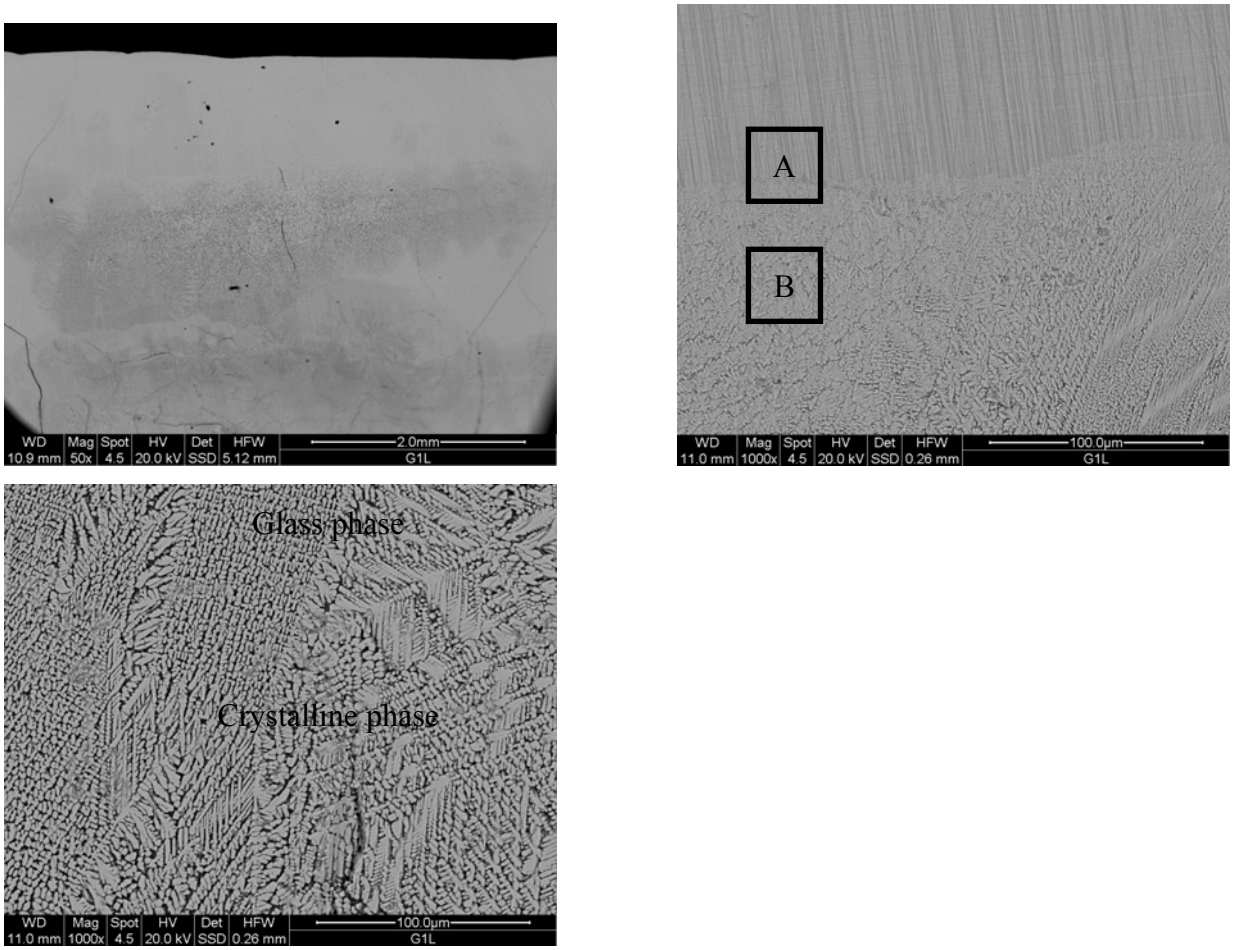

Fig. 8. (a) The broken surface OM image of G1-5L as-cast glass. (b) The SEM cross-section microstructure of G1-5L as-cast glass. (c) This figure is the higher magnification of square A. (d) The figure is the higher magnification of square B.

The results of B4 glass

B4 glass has a few advantages as a sealant. It has suitable T_g (450°C) and T_m (930°C) for intermediate SOFC (650°C). 650°C is the temperature higher than its crystallization temperature. Fig. 9 shows the results of B4 glass after heat-treatment at 650°C holding for 1, 5, and 10 hr. For each condition was taken 15 pictures for residual glass measurement by Image-C program. The value shows above are the average value. The amount of residual glass has no significant change from the 1 hr (9.5 area %) to 10 hr (11.9 area %). It represents that the glass phase stabilized after 1 hr heat-treatment. Only the re-crystallization of Zn_2SiO_4 is more significant. The results of residual glass measurement correspond to the creep behavior in next section.

Fig. 10 shows the wetting behavior of B4 as-cast glass. The results are matched with thermal analysis results. The sample size for this test is really small, so gravity effect can be neglected. The heating rate was 5°C/min. It could be observed that started wetting at 900°C and totally wetted at 990°C. Comparing with G1-glass wetting results, B4-glass has a better wetting behavior on YSZ sintered bulk.

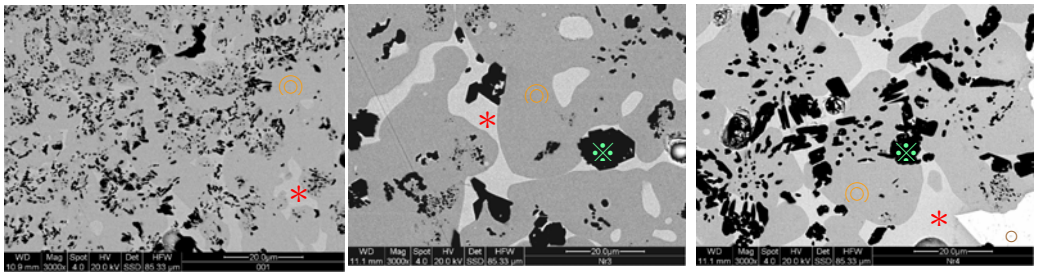

Residual glass: 9.5% (Area%) | Residual glass: 11.5% (Area%) | Residual glass: 11.9% (Area%)

∗: Glass phase ※: Zn_2SiO_4 ◎: $Bi_4Si_3O_{12}$ ○: $Bi_{12}SiO_{20}$

Fig. 9. Results of B4 glass after heat-treatment at 650°C holding for 1, 5, and 10 hr. Each condition was taken 15 pictures for residual glass measurement and calculates average values.

Modified system of G1-glass

G1-glass has a rapidly crystallization character and non-wetting at 1000°C, which is not suitable as a sealant. Literature reported [J. W. Fegus, (2005)] that alumina has the effect to inhabit this rapidly crystallization. So a 10 mol% alumina (the effective amount reported in

literature) added in G1-glass have been tried. To our purpose, a pure glass phase formed by casting method. But the DTA results show the T_g of this glass is higher than 650°C that is a rigid sealing glass. The measurement of others properties will finish in Taiwan.

Creep behavior analysis of G1 and B4 glass

There is no significant shape change (Fig. 5) at 1000°C; we set the temperature at 800°C for creep test. Fig. 11 shows the creep result of G1 as-cast glass with the heating rate of 5°C/min. The first 180 min represents the thermal expansion of glass-ceramic and alumina spacer. From 180 min to 200 min was the sinter behavior of G1 glass-ceramic. The period of 200 min to 280 min showed crystallization and let this glass-ceramics more stable. After 280 min to the end, a creep with the rate 0.12 μm/hr was observed. Integrating the creep behavior with micro-structural results can conclude that G1 is not a suitable glass as a sealant. The characters of this glass are less residual glass phase, less creep behavior at 800°C, and rapidly crystallization. It needs to adjust the composition to overcome these problems. The viscosity can be estimate by eq. (1), and get the apparent viscosity of G1 glass-ceramic is 5.9×10^{12} Pas.

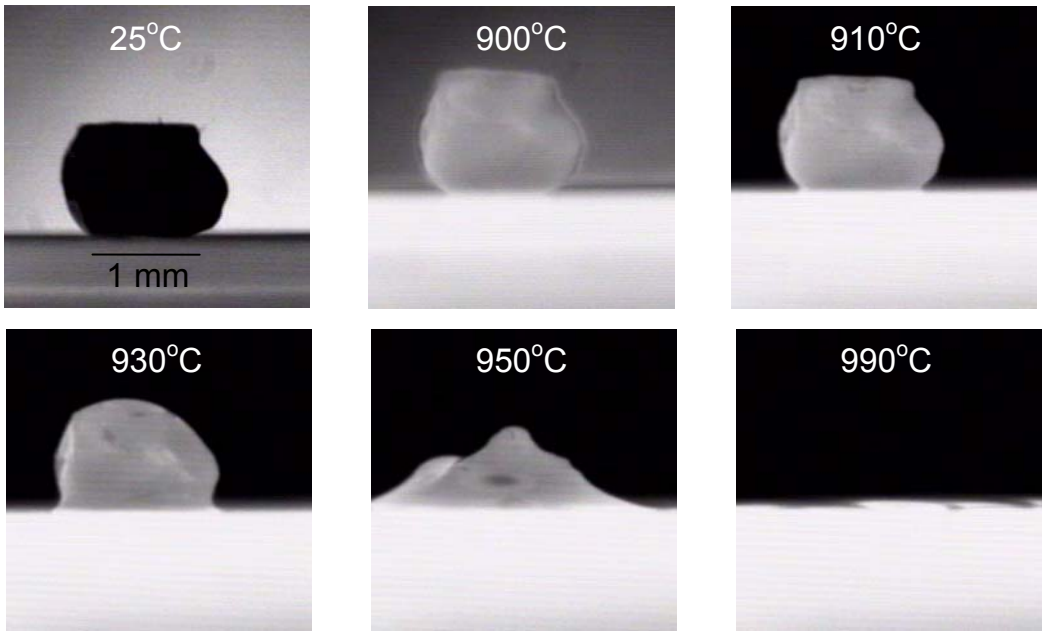

Fig. 10. The wetting behavior of as-cast B4-glass at different temperature. There is starting to wet at 910°C and completely wet on YSZ at 990°C.

Fig. 12 show the morphologies of B4-glass heat-treatment at 650°C holding for different period. Fig. 13 shows the creep result of YSZ/B4/YSZ sample at 650°C with and without load with a heating rate of 10°C/min. The first 60 min is the thermal expansion of YSZ, glass and alumina spacer. There is a deformation at 60 min to 85 min with 8.5 kPa loading. The viscous flow of glass can explain this phenomenon. The crystallization also corresponds to the

heat-treatment, and then the glass becomes a crystal-rich glass-ceramic. So at 85 min, the crystallization is finish (Fig. 12-(b)). After long time heat-treat the creep rates of B4-glass are $3x10^{-3}$ (without load) and $3.3x10^{-3}$ (with load).

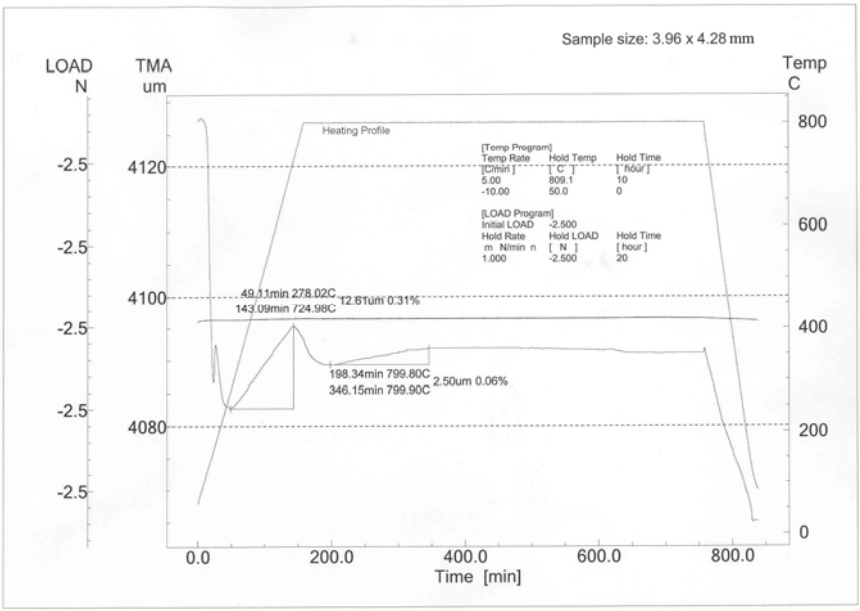

Fig. 11. The TMA result of G1 as-cast glass sample treated to 800°C and held for 10 hr with 5°C/min heating rate. The load is 147 kPa.

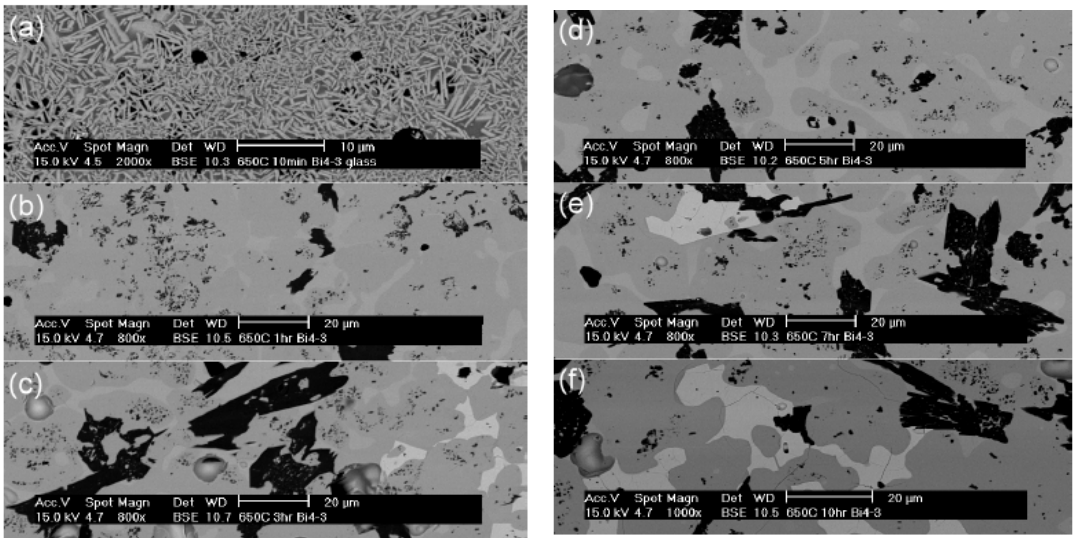

Fig. 12. SEM morphologies of B4-glass heat-treatment at 650°C holding for (a) 10 min, (b) 1 hr, (c) 3 hr, (d) 5 hr, (e) 7 hr, and (f) 10 hr.

Fig. 14 shows the creep behavior of as-crystallized samples with 8.5 kPa loading. Because the samples have been pre-crystallized, there is no observable deformation. The creep rate was proportional to temperature. The viscosity can be estimate by eq. (1). The results of apparent viscosity list in Table 2.

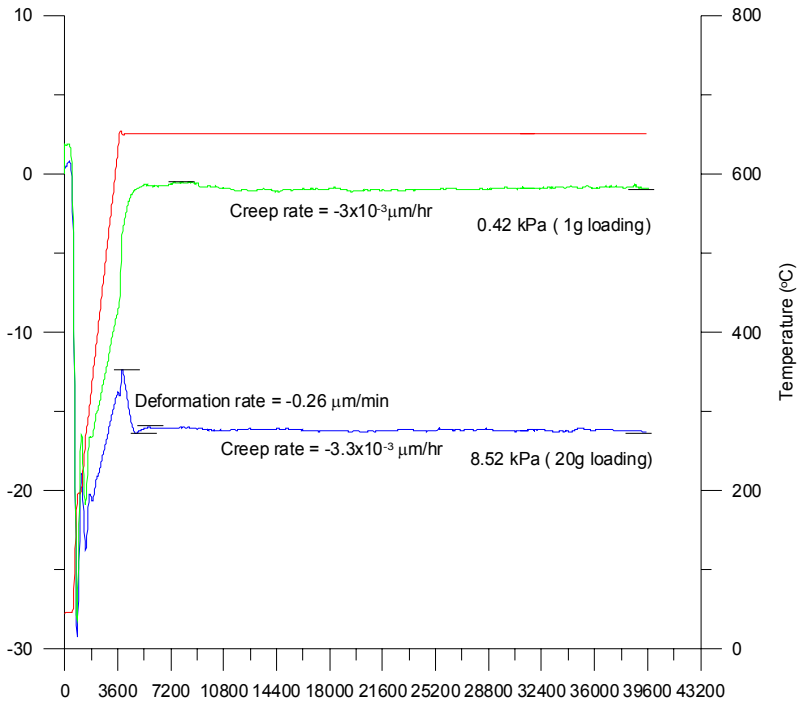

Fig. 13. Creep behavior of YSZ/B4/YSZ samples at 650°C for 10 hr with different load.

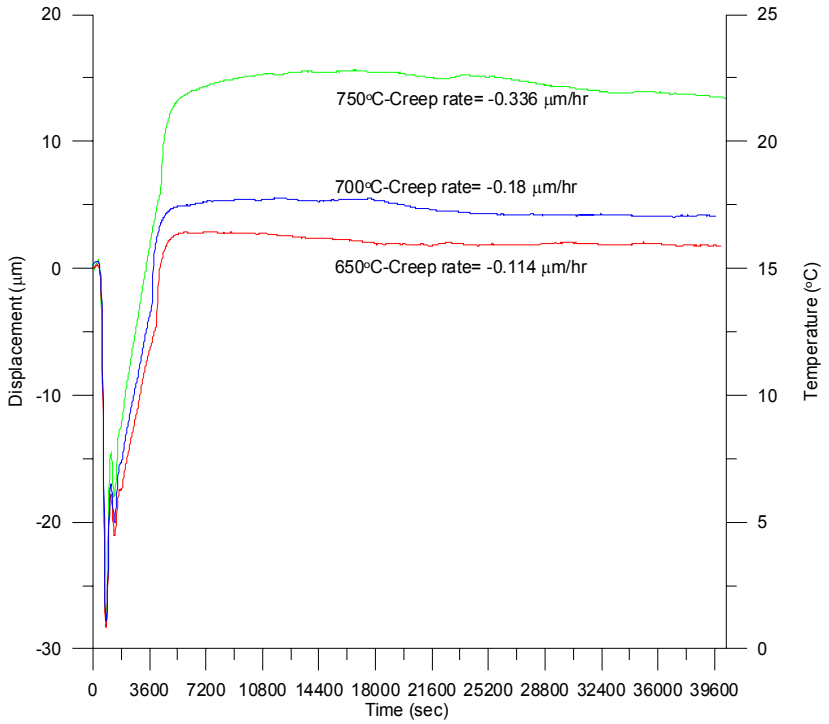

Fig. 14. Creep behavior of YSZ/B4/YSZ samples at 750, 700, and 650°C for 10 hr with different 8.5 kPa load.

Table 2 The viscosity of B4-glass at different heat-treated conditions.

Sample condition	Load (kPa	Apparent viscosity (Pa·s)	Viscosity of glass (Pa·s)
750°C pre-crystallizec	8.5	3.04×10^{9}	3.2×10^{5}
700°C pre-crystallizec	8.5	5.68×10^{9}	6×10^{5}
650°C pre-crystallizec	8.5	8.97×10^{9}	9.49×10^{5}
650°C normal sample	8.5	3.1×10^{10}	3.2×10^{6}
650°C normal sample	0.42	1.68×10^{10}	1.7×10^{6}

The calculations of apparent viscosity are listed in table 2. In these cases, there are no pure glass phase in the sample. The viscosity needs to calculate with the fraction of crystals by using Eq. (3) and (4) with m=-3, f=4.73 (vol. %) [Boccaccini, (1998)]. The results of true viscosity are listed in Table 2. Maxwell relation approach can be calculated to get an accurate value of viscosity from Eqs. (5) and (6). Some experiments are left and still proceeds in Germany. The final results will be available later.

The results of thermal expansion coefficient measurement

Coefficient of thermal expansion (CTE) is an important factor affects the whole sealing condition a lot. The mismatch of CTE will be due to crack formation both inside the

glass and along the joined interface. Table 3 list the CTE measurement results of previous samples. G1 as-cast glass has higher CTE value than YSZ. B4 as-cast glass has suitable CTE value but a long time heat-treatment (crystallization) will decrease it.

Table 3 The CTE measurement results of previous samples

Sample \ CTE	CTE (ppm/K) From R.T. to T_g
G1 as-cast glass bulk	16.7
B4 as-cast glass bulk	10.9
B4 full crystallized sample	4.7
G1-10A as-cast glass bulk	12

The results of composition analysis

Table 4 list ICP results of G1, G1-10A, and B4 glass. A large amount of B_2O_3 lost during the whole melting process. The average loss of B_2O_3 is near to 7 mol% in each glass.

Discussion

After finished the glass casting, wetting behavior measurement, microstructure observation and creep behavior measurement, comparisons of these four glasses are listed in Table 5. B4-glass has several advantages, but the decrease of CTE is the fatal disadvantage. G1-10A has potential as a sealant but still need to lower down T_g.

Table 4 ICP results of G1, G1-10A, and B4 glass

	Bi_2O_3	ZnO	SiO_2	B_2O_3	BaO	Al_2O_3	Na_2O	K_2O	Note
ICP results in mole%									
B4 formula	30.0	20.0	40.0	10.0					200°C melt, held
Result	**31.7**	**20.0**	**44.7**	**3.5**			**0.1**		min, 3 times
G1 formula			28.0	22.0	50.0				200°C melt, held
Result			**30.2**	**17.3**	**52.5**		**0.0**		hr, 1 time
G1-10A formu			25.5	20.0	45.5	9.0			400°C melt, held
Result			**28.4**	**12.5**	**49.6**	**9.5**	**0.1**		hr, 1 time

Table 5 comparisons of different sealing factors with G1, G1-5L, G1-10A and B4 glass.

	G1	G1-5L	G1-10A	B4
Glass formation	Rapidly crystallization, n higher cooling ra	Inhomogeneous crystallization, still have chanc application	Easy formation	Easy formation
T_g (glass trar temperature)	550°C, lower 650°C	lower than 650°C	Higher than 650°	450°C, lower 650°C
CTE	Too high to use	N/A	Suitable application	Crystallization c large decrease of
Wetting behavi YSZ	Non-wetting	N/A	N/A	Good wetting

5. Conclusions

- The properties of G1-glass that has rapidly crystallization and non-wetting on YSZ. It is not a suitable material as a sealant. The creep behavior of this system at 800°C is also small, which is caused by small amount of glass phase.
- G1-10A glass has a match CTE and easily form pure glass. It has potential as a sealing material.
- B4-glass has several advantages such as good wetting behavior, easy formation, better creep behavior and suitable T_g. CTE is the fatal disadvantage of this system. Maybe it could be modified by adding with ceramic powder (composite) to adjust its character.
- Following the ICP results that the content of B_2O_3 lost 7 mol% to 9 mol% during the glass casting process.

6. Proceeding work

Two experiments are contiunous in Germany:

- The analysis of HT-XRD the crystalline phase of G1, G1-10A, and B4 glass.
- Cyclic load TMA measurement of G1-glass and as-cast G1-glass for Maxwell relation analysis.
-

Reference

1. H. Rawson, "*Properties and Applications of Glass*", Elsevier, 1980
2. M. Koide, R. Sato, T. Komatsu and K. Mazumasa, "Viscosity and relaxation of glasses below the glass transition temperature", Thermochimica Acta, 280/281, 401-415 (1996).
3. L. Heymann, E. Noack and L. Laempfe, "An experimental study on the influence of shear on the flow behavior, spontaneous crystallization, microstructure and mechanical properties of a fluorophlogopite glass-ceramic", Mat. Sci. Eng., A196, 261-273 (1995)
4. J. S. Reed, "*Principle of Ceramic Processing*", Wiley Inter. Science, 1994.
5. N. V. R. Kumar, S. Prinz, Y. Cai, A. Zimmermann, F. Aldinger, F. Berger and K. Muller, "Crystallization and creep behavior of Si–B–C–N ceramics", Acta. Materialia, 53, 4567-4578 (2005).
6. A. R. Boccaccini, "On the viscosity of glass composites containing rigid inclusions ", Mat. Let., 34, 285-289 (1998).
7. P. Z. Cai, G. L. Messing, and D. L. Green, "Determination of the mechanical response of sintering compacts ", J. Am. Ceram. Soc., Vol. 80, 445 (1997).
8. J. W. Fegus, "Sealants for solid oxide fuel cells", J. Power Sources, 147, 46-57 (2005).

2007 氫及燃料電池會議

報告人: 台大材料系 韋文誠

會議期間: 4/29-5/2/2007，加拿大溫哥華市

一、參加會議經過

H_2 and Fuel Cell 2007 今年在溫哥華召開，由加國 Hydrogen & Fuel Cell 委員會主辦，邀請來自 35 國家專家及學者參加。這是筆者過去參加的會議中最多環保及綠能公共政策制定及執行人員參加的會議。

會議主題環繞在氫能及燃料電池的主題下進行，加國執行的氫能及燃料電池計畫尋求全球夥伴及合作關係(Company ship, partnership and collaboration)。爲推廣綠能觀念，也邀請電池及氫能生產廠商參加，加國產業界(約有四十五家公司)、官方(卑詩省省省長及加國環能主管)、及民間團體，共一百餘個單位共同參與。

會議所在地的加拿大卑詩省(British Columbia)省長及國家省級環境及綠能主管均列席報告加拿大投入的資源與願景，並願承擔其國際公民應盡的責任。

歐洲主要參加國有德國、丹麥、荷蘭，挪威及鄰國美國的聯邦環境主管、加州主管環境主管都與會並致詞。

會議由 4/29 晚上開始，共舉行三天，除了有約二十餘場邀請演講，其他學術性及通俗性演講有八、九十場次，則分成七、八個場地同時舉行，相當熱鬧。會議期間也有 trade show，主要是加國氫能產業，共三、四十家公司，還包括非營利團體，展示他們的成果，大部分的內容都是最新成果，很值得收集。

會間，主辦單位之一 NRC 也開放其在溫哥華的研究所(institute of fuel cell innovation)，供與會人士分批參觀。另外，也有兩個成功應用燃料電池的公司，Cellex power 及 Westport innovation，由主辦單位接洽，開放參觀。

演講主題中有幾個主題相當前瞻及重要，一是替代能源公共政策，一是現有推動氫能使用範例介紹，一是固態電解質燃料電池技術發展，最後是 PEM 燃料電池技術發展。

二、與會心得

2.1 加拿大國能源使用經歷

1904 第一輛車到溫哥華，1907 僅成長到兩百輛車，第一個加油站在此年成立。目前加國在 OECD 組織之中產氫量最高，每年爲 3M tons。相關產業 2005 年雇用人有 1902 人，R&D 經費加幣 218M，收益$135M，過去五年加拿大已投資 10 億加幣在氫能及燃料電池項目。

加國最好的大學 Univ. BC 提供能源實驗室訓練，2010 冬季奧運 20 輛 FC 巴士車隊加入維多利亞(Victoria)->溫哥華>Whistler 間的交通。更進一步，加國與美國及墨西哥，由北至南，建立 hydrogen highway，今年投入$85M 經費 與美國加州連成一線。卑詩省省長提出期望 ”需要改變使用能源之習慣及態度及提升科技”。

環境部 Dr. Rose 報告加國環境及能源政策的發展，都會區因爲私人車輛增加，人口集中，廢氣排放等比增加。碳能消耗及京都議定書對於二氧化碳之限制，簡單的能源使用關係如下：

每增加燃料電池組 3 kW/year 及相當於節省兩輛 2000 cc 汽車/year 的用油量。

對應綠色能源，政策上增加汽油稅，減低燃料電池技術發展稅額，補助技術發展措施，政策鼓勵使用生質能源。目前能源使用，以發展較佳的電池，配合天然氣(nature gas)的使用，可以減少-64%碳量。短期進口汽電共用汽車，給予免稅，生產較佳電池等等。中期使用生質燃油，遠期使用氫能及核能。對於未來 ” Challenge is not easy, but they are hard. They are much to do”

加國二氧化碳產生來源：工業 17%，運輸佔 21%，發電佔 40%。

2.2 美國

Freeman 博士 [NASA]採用太空精密量測技術 得知大氣中污染氣體及水分精確數據，證實氣候確實因爲空氣污染而改變。

加州 Vedugo-Peralta 女士報告該州相關之政策(2004/4 簽署 CA H_2 highway network)及成效。數據顯示因大氣層污染，導致加州每年七萬人次生病，兩萬四千早產兒，已是明顯的負擔。該州將 05/06 投入 US$6.5M 進行示範型計畫，其中 $3.7M 建置氫氣站。06/07 投入$5M 購置五輛巴士。

2.3 德國氫能及燃料電池之投入

Garche 博士報告德國的努力都涵蓋在綠能技術及應用主題，1975-2000 每年投入 600 萬歐元進行 R&D，2001-2005 進行 R&D 及示範，2006-2015 預定投入 2097M 歐元(目前僅有 1400M 歐元預算)，其中 2/3 進行示範及建立周邊基礎設施(demonstration and establish infrastructure)，1/3 投入 R&D 中。

分配如下：運輸 1100M 歐元，住宅用燃料電池(residential，3 kW 左右)佔 500M 歐元，工業用燃料電池(100 kW-250 kW)佔 250M 歐元，特殊市場 220M 歐元。

預估燃料電池成長 2010 年 54MW，2015 年成長到 620MW。電力轉換效能高於 35%，整體能源使用效率高於 90%，使用壽命 25000 小時，成本 3000 歐元/kW。

2.4 日本投入

短期(2002-2010) 建立 infrastructure, codes, R&D，研究重點 FC 車輛的電池系統改善，高效能鋰電池，定置型 PEMFC(1 kW 型)。

中期(2010-2020)及長期(2020-2030)等等。

2.4 歐盟

Paulmier 博士報告歐洲 Hychain-minitrains 計畫。24 夥伴(partners)在 2006/01 簽署三個階段(phases)發展 158 輛氫能車之計畫，初期發展電動車輛及周邊設備，包括三輪腳踏車(圖 1)40 輛，輪椅(0.35 kW)34 輛，速克達(2.0 kW) 40 輛，送貨車(2.5 kW)44 輛，迷你巴士(10 kW)10 輛。

挪威人口 450 萬人，90%電力來自水力發電，第一輛車(Benz)在 1895 年登陸。目前氫能公路延著半島南部每隔約 200 公里建置氫氣加油站，第一個在 Sotavanger 市建立，分成兩種氫氣壓力(350 及 700 bar)，加油站也能加入 NG，混和氣共七種氣體。該國未來 2010-2020 著重在氫氣合成與分銷，氫氣車輛商業化市場，主要優先項目：國際合作，生活示範(real life demonstration)，增加國家級測試及 R&D 中心，期望每年能吸引 US$200M 投資。

圖 1 歐盟發展之兩種展示的氫能車輛。

2.5 汽車業報告

Bill Reinert (Toyota)報告汽車用燃料電池只能接受 15 kg，35-70 kW 電池組，攜帶燃料可以行駛 300-500 km，這樣的需求 2030 以後才有可能達成。

GM 在 2004 產製氫能車(HydroGen 3)具有 130 kW，1.64 kW/lit 效能。

日產最近一個 X-trail 車型(圖 2)，其放置氫氣儲存槽，鋰電池，驅動馬達及轉化器(invertor)位置接近最佳化。

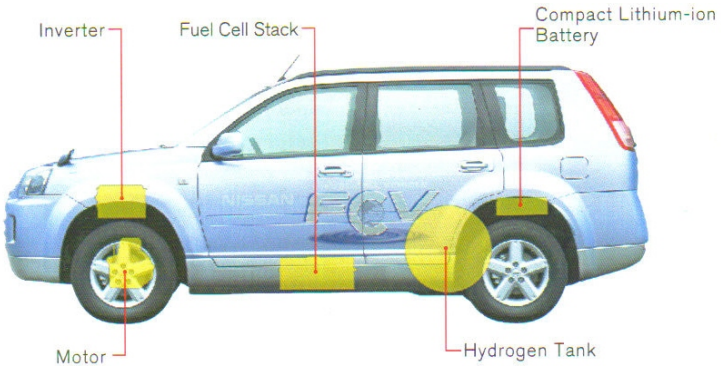

圖 2

2.6 學術界報告

Dr. Sarka (Alberta Research Council) Micro-open micro-tube FC stack, 微管由電泳法製作 多層管可以數分鐘電泳鍍膜完成，緻密電解質層約爲 2 微米，能量密度 0.7 V 440 mW/cm^2，2 kW/litter, 使用玻璃陶瓷封裝，電極厚度小於微米，陽極電阻較高。

Berghaus 博士報導電漿噴塗氧化铈(SDC)層在 16x16cm^2 陽極上，厚度 20 μm，晶粒大小爲 40 nm，在 650°C 操作，得到 0.22W/cm^2 輸出效能，

三、參觀活動

大會工安排兩項參觀活動

3.1 National Research Council (NRC) IFCI 實驗室

位在溫哥華市郊，與 UBC 一起，約三十分鐘車程。目前有 110 位研究及一般人員，加國最大之氫能及人料電池研究團体，包括材料製程、模擬、測試等五研究團隊。

主要的建築物分成兩部分，前半部爲一般辦公區，有地面熱源，屋頂之太陽能，後半部爲燃料電池研究區域，PEMFC 佔 60%，SOFC 佔 30%，氫能 10%。

建築物外面有測試實驗室(以貨櫃箱爲架構，如下圖 3) 進行各種環境測試，FC 車輛停放保養區(圖 4)，及示範加氫站之區域(圖 5)。

圖 3 室外氫氣安全測試站。

圖 4 加國 IFCI 研究中心之第一代 FC 巴士(BMW)及轎車(Ford)

氫能技術由下列幾實驗室執行

1. 氫氣安全實驗室(室外)
2. 燃料電池汽車(FCV)之保養區
3. 電解質
4. 環境測試櫃(environmental testing chamber)
5. 加氫站 (Pacific Spirit)
6. 氫氣儲存槽

圖 5 加氫設備及儲存裝置。

SOFC 幾項重要研究主題，RSDC technology(反應噴塗沉積電解質技術)，目前以<600℃ 操作溫度爲目標。

PEMFC 採用 1kW stack 實用化，共有 18 大學 85 研究人員 14 公司合作。

3.2 Cellex power 及 Westport innovation 私人公司參觀

Cellex power 主要在應用燃料電池組，裝置在搬運用堆高機，並設置安全可靠的氫氣添加站，將此氫能設備發揮功能，自 2002 起受到多家知名物流業(包括 Wal-Mart)的青睞，改換鉛酸電能組件爲氫能燃料電池，效益明顯。

Westport 也是新成立的公司，主要的專攻項目是改裝重型大貨車的引擎噴入燃料系統，使用液態瓦斯及一定量氫氣，或是全氫方式噴入引擎燃燒室中燃燒，可一大幅減少才由引擎排放之廢氣，

四、心得

1. 看到全球綠色能源展望(Global View)。
2. 加拿大之氫能工業、卑詩省(British Columbia)、科技研究三方合作努力之成效。
3. 國際燃料電池主要國家最近發展及承諾，包括美國、德國、日本、挪威、丹麥。

五、攜回資料

1. Canada’s Fuel Cell and Hydrogen Industry, 04/05 Capabilities Guide
2. Canada’s Hydrogen + Fuel Cell Industry 2007 capabilities Guide